



Recent advances on nanocellulose-graphene oxide composites: a review

T. C. Mokhena · M. J. Mochane · A. Mtibe ·
S. Sigonya · B. Ntsendwana · E. G. Masibi ·
L. Sikhwivhilu · T. S. Motsoeneng

Received: 21 December 2023 / Accepted: 6 July 2024 / Published online: 15 July 2024
© The Author(s) 2024

Abstract Nanocellulose (NC)/graphene oxide (GO) composites are attractive materials with a range of unique features obtained from the integration of NC and GO. These materials have high potential use in various sectors such as biomedicine, wastewater remediation, sensor/biosensor technology, and energy storage/conversion. The simple functionalization and modification of NC or GO afford an opportunity for tailoring these materials for anticipated applications. In wastewater treatment applications, they can be employed as reliable adsorbents for the removal of

different pollutants, such as metals, dyes, oils, and pesticides as well as sensors for the detection and monitoring of these pollutants. Besides that, NC/GO composites can be applied as catalysts for catalytic degradation for a wide variety of pollutants. These materials have been also reported to be applicable in biomedical applications such as drug delivery, antibacterial and biosensing. Energy storage applications such as supercapacitors NC/GO-based materials were also utilized. This review summarizes NC/GO hybrid fabrication, characterization, and their application in different fields, i.e. sensing, energy storage, and wastewater remediation. It also covered a broad overview of the status of integrating GO with nanocellulose materials, i.e. bacterial cellulose, cellulose nanofibrils, and cellulose nanocrystals. We concluded with the challenges and outlook for NC/GO-based composites.

T. C. Mokhena (✉) · S. Sigonya · B. Ntsendwana ·
E. G. Masibi · L. Sikhwivhilu
DSI/Mintek- Nanotechnology Innovation Centre,
Advanced Materials, Mintek, Randburg, South Africa
e-mail: mokhenateboho@gmail.com

M. J. Mochane
Department of Life Sciences, Central University
of Technology Free State, Bloemfontein, South Africa

A. Mtibe
Centre for Nanostructures and Advanced Materials,
DSI-CSIR Nanotechnology Innovation Centre, Council
for Scientific and Industrial Research, Pretoria,
South Africa

S. Sigonya
Department of Chemistry, Durban University
of Technology, Durban, South Africa

T. S. Motsoeneng
Department of Chemistry, University of Zululand,
KwaDlangwezw, South Africa

Keywords Graphene oxide · Nanocellulose ·
Hybrids · Biosensing · Energy storage · Wastewater
remediation

Introduction

The interest in nanocellulose materials continues to rise due to their unique and advantageous properties, such as renewability, biocompatibility, biodegradability, high aspect ratio, low thermal expansion, and remarkable mechanical properties (Mokhena

and John 2020a). In addition, facile chemical modification through –OH groups is one of the greatest strengths enabling optimized versions of these biomaterials to be preferable for various applications, such as wearable electronic devices, sensors, sorbent materials, cosmetics, packaging materials, and biomedical. The employed isolation process also affords cellulose materials with different dimensions that can further be processed to the desired form (e.g. three dimensional (3D) materials, hydrogels, aerogels, etc.) depending on the intended application.

Nanocellulose can be derived from different sources, such as wood (softwood and hardwood) (Yousefi et al. 2018), non-woody sources (bamboo, banana stalks, coir, cotton (Uddin et al. 2011), garlic (Prasad Reddy and Rhim 2014), grass, hemp, maize stalks, pineapple, ramie (Peresin et al. 2010), rice stalks, sisal (Garcia de Rodriguez et al. 2006) and soy hulls (Flauzino Neto et al. 2013) and tunicates (Anglès and Dufresne 2000). Moreover, organisms such as algae (e.g., *Gelidium elegans*) (Chen et al. 2016b; El Achaby et al. 2018) and bacteria (Roman and Winter 2004) (e.g., *Komagataeibacter*, *Rhizobium*, and *Sarcina*) can synthesize cellulose. Other sources that can be used for nanocellulose isolation include *Chamaecytisus proliferus* (Espinosa et al. 2017), fibre sludge (Mautner et al. 2016), fungi (Ifuku 2014), *Leucaena leucocephala* (Espinosa et al. 2017), old newspapers (Campano et al. 2017), old corrugated containers (Tang et al. 2015), paper mill sludge (Du et al. 2020), wastepaper (Danial et al. 2015) and water hyacinth (Marimuthu and Atmakuru 2015; Thiripura Sundari and Ramesh 2012). These sources have been used as one of the methods to categorize nanocellulose materials, viz. woody, nonwoody, agricultural waste, tunicate, bacterial, and algal cellulose. Furthermore, the dimensions of the nanocellulose have been employed as an alternative method for categorizing nanocellulose materials, namely cellulose nanocrystals (CNCs), spherical nanocellulose (SNC), cellulose nanofibrils (CNFs), or microfibrillated cellulose (MFC) (Ayissi Eyebe et al. 2017). In this review, all cellulose materials with one dimension in nanometre will be referred to as ‘nanocellulose’ throughout the manuscript, unless otherwise stated. The classification of the nanocellulose or cellulose nanomaterials are covered in these reviews for interested readers (Trache et al. 2020; Foster et al. 2018). Beyond chemical modification, nanocellulose has

been mixed with other nanomaterials to broaden their applications (Oun et al. 2020). The presence of these nanomaterials not only enhances the functionality of the resulting hybrid materials, but also improves the overall properties which broaden their application in various fields (Yousefi et al. 2018; Wang et al. 2015; Oun et al. 2020). It is worth noting that the preparation method used and the ratio of the components play essential roles in the resulting properties of the hybrid materials (Oun et al. 2020). Wang et al. (2015) studied a comparison between multifunctional graphene nanoplatelets/cellulose composite prepared with and without melt-pressing process. It was reported that 15wt% CNC exhibited the best in-plane thermal conductivity of $\sim 47 \text{ Wm}^{-1} \text{ K}^{-1}$ and $\sim 73 \text{ Wm}^{-1} \text{ K}^{-1}$ for non-pressed and melt-pressed films, respectively. Amongst the nanomaterials exploited, graphene-based materials are of interest due to their unique 2D structures.

Graphene is one of the cheapest carbonaceous materials. It is a highly reactive material due to the available surface functionalities, viz. –OH, epoxy, and carboxylic groups (Jiao et al. 2022). These groups can be exploited to impose additional functionality or mixed with other nanomaterials to achieve the desired functionalities. A recent study by Nizam et al. (2020) demonstrated that amino-functionalized graphene oxide/nanocellulose can be exploited to prepare mechanically robust antibacterial nanopapers for the removal of different pollutants from water. The resulting paper exhibited high antibacterial activity against *E. coli* MTCC and *Klebsiella* with good dye removal efficiency. In addition, the modification of graphene is often carried out to promote interfacial adhesion with nanocellulose materials (Sadasivuni et al. 2015). The interfacial adhesion between nanocellulose and graphene-based materials plays a critical role in the ensuing properties. Polyethylene glycol (PEG) functionalization of graphene resulted in the formation of hydrogen bonding between nanocellulose and graphene resulting in better alignment of graphene nanosheets for enhanced thermal conductivity and superior mechanical performance (Jiao et al. 2022).

This review article summarizes the most recent advancements and achievements in CNF/GO hybrid composites. It covers the fundamental processes often employed for the isolation of nanocellulose and the synthesis of GO for their usage in the preparation of CNF/GO hybrids. It will discuss the applicability

of CNF/GO hybrids in various fields, such as water remediation, sensing, and energy storage. These materials were applied in wastewater treatment for the adsorption of different pollutants (dyes, oils, and emerging pollutants). They were applied in energy storage (super-capacitors) and sensing applications. The benefits and disadvantages of using these materials will be elucidated. Lastly, it will cover the challenges and prospects of CNF/GO hybrid materials.

Cellulose sources

Cellulose has found application in many areas because of its distinctive attributes such as biocompatibility, biodegradability, abundant availability at low cost, renewability, lightweightness, and excellent mechanical performance (Ayissi Eyebe et al. 2017; Pennells et al. 2020). It is a naturally occurring polysaccharide composed of glucose units (> 10 000) linked together via β -(1–4)-glycosidic bonds. The presence of hydroxy (–OH) groups along the chains result in the formation of hydrogen bridges and thus fibrillary structure. The exploitation of the –OH groups for surface chemical modification gives cellulose a competitive edge that enables its optimization to afford preferable biomaterials for a wide variety of applications.

Cellulose is the most abundant polymer on earth that can be obtained from various sources, such as woody, non-woody, and animals (Roman and Winter 2004). This has resulted in researchers broadly classifying cellulose according to the source, i.e. woody or non-woody (plant), algal, tunicate, and bacterial cellulose. In woody and non-woody sources, cellulose is embedded within lignin and hemicellulose with other extractives. A wide variety of treatments are employed to remove other constituents (i.e., lignin, hemicellulose, pectin, and extractives) than cellulose.

Algal cellulose has less lignin which makes it preferable as a complementary cellulose source (Tarchoun et al. 2019; Bettaieb et al. 2015). This simplifies the isolation of cellulose from algal biomass and reduces the overall cost of extracting lignin and hemicellulose, which is generally higher for lignocellulosic sources. It has a high growth rate with a simple cell structure when compared to plant-based cellulose (Tarchoun et al. 2019; Bettaieb et al. 2015). Algal cellulose has cellulose I α crystal structure which is similar to bacterial cellulose (French 2014; Nishiyama et al. 2003,

2002). Bacterial cellulose is the purest form of cellulose with excellent strength and water-holding ability (Jiang et al. 2019). In this case, bacteria produce cellulose under suitable conditions. Bacteria produce cellulose using low-molecular-weight sugars as a food source. The as-produced cellulose through biochemical steps is obtained as entangled three-dimensional (3D) network hydrogel (Jiang et al. 2019). Bacterial cellulose is chemically and structurally similar to algal cellulose, with ultrathin fibrils having diameters ranging between 80–150 nm. Tunicates (small marine animal) is another source of cellulose. Tunicate cellulose is highly pure and often highly crystalline due to the absence of lignin, hemicellulose, and pectin (De Souza Lima et al. 2003). These include *Styela clava*, *Ciona intestinalis*, *Microcosmus fulcatus*, *Styela plicata*, *Ciona intestinalis*, and *Halocynthia roretzi*. The main processes employed for the isolation of cellulose from the tunicate skeletal structure are acid pre-hydrolysis and bleaching (Yadong Zhao and Li 2014). The resultant cellulose has the cellulose I β structure similar to high plant cellulose (French 2014; Nishiyama et al. 2003, 2002).

Nanocellulose

As mentioned earlier, different cellulose sources can be utilized to fashion nanocellulose materials (Mtibe et al. 2018). These materials can be treated either mechanically (Dunlop et al. 2018) or chemically (Barbash et al. 2016), as secondary treatments, to produce nanocellulose particles. It has been recognized that these treatments can be combined to produce nanocellulose particles with desired dimensions and physico-chemical properties. The obtained nanocellulose particles with different dimensions can be categorized according to their sources, viz. algal, tunicates, woody (Mokhena and John 2020b; Boufi 2017), non-woody (Mokhena and Luyt 2014; Boufi and Chaker 2016) and bacterial. In recent years, agricultural-based fibers have attracted great interest to complement traditional fibres and wood as a cheaper, renewable, and abundantly available source of cellulose (Boufi 2017). In addition, nanocellulose or cellulose nanomaterials (CNMs), are classified according to their dimensions as cellulose nanocrystals (CNCs), spherical nanocellulose (SNC) (Fattahi Meyabadi et al. 2014) and cellulose nanofibrils (CNFs) or microfibrillated

cellulose (MFC). The dimensions directly dependent on the preparation/isolation methods employed. Cellulose nanocrystals (CNCs) can be recognized by their rod-like structure with cross-sections between 3–5 nm and lengths of up to 3 μm . The most common used method for preparing CNCs is acid hydrolysis of pure cellulose material. These acids often introduce different surface functionalities depending on the acid used (Rwegasila et al. 2024). Sulphuric acid, for instance, introduces sulphate groups (SO_4^{2-}) into the nanocellulose, while phosphoric acid introduces phosphates (PO_4). The use of malic acid has been reported in the literature as one of the green methods for isolating nanocellulose resulting in particles decorated with maleic acid groups. The reason for the resulting crystallites is the high susceptibility of the amorphous regions to hydrolytic effects compared to the crystalline parts.

Cellulose nanofibrils (CNFs) are long web-like flexible particles with diameters between 5–60 nm and lengths of $> 1 \mu\text{m}$ (Barbash et al. 2016; Mokhena and John 2020b; Boufi and Chaker 2016). These materials are often obtained through mechanical, chemical, and enzymatic treatments of pure cellulose (Xu and Chen 2019; Beltramino et al. 2018; Teixeira et al. 2015; Hernández-Becerra et al. 2023; Hwang et al. 2024). Mechanical methods involve high shear forces that reduce the size of the cellulose fibres to nanoscale particles (Hernández-Becerra et al. 2023; Van Hai et al. 2018; Teixeira et al. 2015). The high energy consumption associated with mechanical methods is one of the main problems in the production of nanocellulose using these methods. Chemical methods involve the cleavage of 1–4 glycosidic bonds of the cellulose chains to obtain highly crystalline nanoparticles through elimination of amorphous regions (Barbash et al. 2016). On the other hand, the enzymatic process is time-consuming and requires the use of expensive reagents to enable the biosynthesis of monosaccharides or the fermentation of cellulose. Therefore, chemical and enzymatic processes are often used prior mechanical treatment in order to reduce the overall energy consumption during fibrillation.

SNCs are often produced by acid hydrolysis of cellulose material from a mixture of acids. These particles range from 5 to 570 nm in diameter (Zhang et al. 2007; Fattahi Meyabadi et al. 2014; Lu and Hsieh 2010). It was reported that prior swelling of the

cellulose source in dimethyl sulphoxide (DMSO) and sodium hydroxide (NaOH) followed by acid hydrolysis in a sonicator leads to the production of spherical nanocellulose (Lu and Hsieh 2010; Zhang et al. 2007). Fattahi Meyabadi et al. (2014) reported on the preparation of the spherical NCs using the green method, viz. enzymatic hydrolysis and sonication treatment, as shown in Fig. 1. It was reported that the resulting spherical NCs, which were less than 100 nm in diameter, were thermally stable. This is due to the absence of sulphates groups on the surface of the nanocellulose which often originate from the conventional sulphuric acid hydrolysis process. Enzymes attach to the cellulose chains. Cellulbiohydrolase and endoglucanase attack crystalline and amorphous regions respectively. Enzymatic hydrolysis reduces the length of cellulose chains by cleaving the of β -D-(1,4)f-glycosidic linkages. As mentioned earlier, the concern with enzymatic hydrolysis are the expensive reagents and time consumption. However, sonication can further reduce the chain length of cellulose (Fig. 1e).

Apart from the fact that nanocellulose is chemically similar to bulk cellulose, the resulting nanoparticles have distinctly different properties, such as high water retention, excellent mechanical performance, highly crystalline etc. These properties often depend on the source, the surface chemistry, and the isolation process, as reviewed in Table 1. For example, nanoparticles derived from tunicates and bacteria have larger nanocrystalline particles compared to particles derived from wood (Zhang et al. 2007). The isolation process also has a significant effect on the size, morphology and surface functionality of the resulting particles. Reviews with detailed methods for the isolation of nanocellulose are available in the literature (Teo and Wahab 2020; Mokhena and John 2020a; Oun et al. 2020; Pennells et al. 2020; Wang et al. 2021a).

Graphene

Carbonaceous nanomaterials are recognized for their extraordinary properties, hence being employed in every application (Iijima and Ichihashi 1993; Zhang et al. 2017; Mokhena et al. 2022). Various techniques/methods and sources are employed to produce carbon-based materials with different functionalities, dimensions, and aspect ratios. Carbon nanomaterials

Fig. 1 (a) Attachment of cellulase enzyme to cellulose fibrils, (b) enzymatic hydrolysis shortening the cellulose by breaking the β -D-(1,4) glycosidic linkages, (c) hydrolysis weakening the hydrogen bonds within the cellulose structure, (d) further hydrolysis significantly reducing the degree of polymerization, and (e) sonication converting the hydrolyzed fiber particles to approximately 70 nm. Reproduced with permission from (Fattahi Meyabadi et al. 2014)

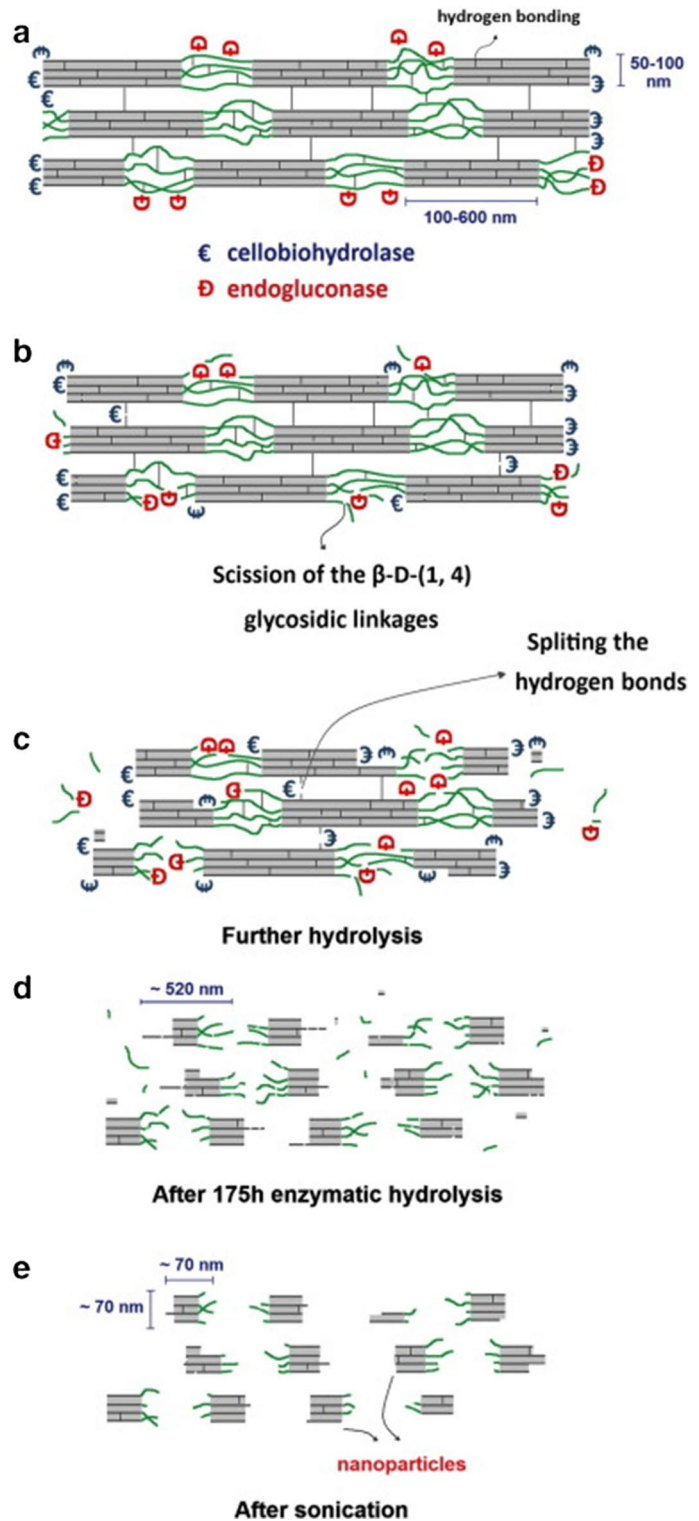


Table 1 Properties of nanocellulose from different sources

Source	Synonym	Shape	Pre-treatment	Post-treatment	Cross-section (nm)	Lengths	Aspect ratio	Crystallinity (%)	Refs
Sisal fibre	Nanocrystals	Rod-like	Alkali	Acid hydrolysis + Sonication	12	197 nm	16	~ 89	(Mokhena and Luyt 2014)
Cotton	Nanocrystals	Spherical	Enzymatic	Sonication	70–200	-	-	~ 79	(Fattahi Meyabadi et al. 2014)
Sawdust	CNFs	Web-like	Alkali	Mechanical grinding	2–28	Few microns	-	~ 70.5	(Mokhena and John 2020b)
Corn stalk	CNFs	Web-like	Soxhlet extraction + TEMPO	High speed blender	4–5	200 nm to Few microns	-	-	(Boufi and Chaker 2016)
Bleached Kraft pulp	CNFs	Web-like		High pressure homo	12–18	Few microns	-	68–75	(Hernández-Becerra et al. 2023)
Softwood bleached Kraft pulp	CNFs	Web-like	-	TEMPO + aqueous counter collision	18.4–22.0	652–850	43–45	66.5–70.1	(Van Hai et al. 2018)
Hardwood bleached Kraft pulp			-		15.1–17.5	815–992	43–49	63.8–71.7	
Eucalyptus pulp-board	SNCs	Spherical particles	-	Enzymatic	15–40a	-	55.8	-	(Xu and Chen 2019)
Banana rachis	CNFs	Web-like	Alkali/hydrogen peroxide	Acid hydrolysis + Sodium nitrite	5.3	1231	-	70.7–99.9	(Rwegasila et al. 2024)

a = diameter

with their morphologies of different dimensions can be classified as either 0D (fullerene), 1D (nanofibers and nanotubes), 2D (GO and graphene nanoplatelets) or 3D (graphite, diamond, and carbon black) (Mokhena et al. 2022; Basu and Bhattacharyya 2012; Yan et al. 2019; Tsai and Tu 2010; Verma et al. 2019). These morphologies can be achieved through the production method and the precursor used. Graphene, as a 2D carbonaceous material, is attracting great interest from industrial and research communities due to its attractive properties, such as high thermal stability, excellent chemical stability, high electrical conductivity, high thermal conductivity, and remarkable mechanical performance. These properties

can be tailored by changing from 2 to 3D graphene (Zhao et al. 2014; Yavari et al. 2011). Several studies reported on the fabrication of 3D graphene through CVD with the aid of a template (Zhao et al. 2014; Yavari et al. 2011). Porous 3D graphene was first prepared using nickel foam as a template, and catalyst and methane as carbon source to afford an interconnected structure with a surface area of $\sim 850 \text{ m}^2 \text{ g}^{-1}$ (Yavari et al. 2011). The porosity can be tailored by changing the nickel foam and the number of graphene layers directly depends on the methane concentration and thus the surface area of the resulting 3D graphene structure. Changing the carbon source and template as well as the concentration of the carbon source

offers possibility to synthesize the desired graphene structure and, thus tailor the properties to the desired applications.

Nevertheless, methods that are usually employed for synthesis of other carbonaceous nanostructured materials, have been used for the preparation of graphene, such as mechanical exfoliation, and ion exfoliation (Lee et al. 2008). In addition, graphene can be exfoliated from oxidized graphite. The oxidation process weakens the interlayer bonding between the graphite layers so that graphene can be produced. This synthesis process of graphene layers was discovered by Andre Geim and Kostya Novoselov, who were later awarded the Nobel Prize in 2010. Graphene consists of a single sheet of graphite. This layer has a thickness of ~ 0.35 nm and consists of carbon atoms arranged in a hexagonal lattice. The obtained graphene can then be reduced to GO via thermal or chemical methods. GO is one of the most important graphene derivatives with hydrophilic groups, such as epoxy, carbonyl, and hydroxyl (Kim et al. 2021). These functionalities are located on the basal planes and edges of GO sheets making them easily dispersed in commonly used polar solvents. Since it is derived from graphite via chemical exfoliation, GO is the cheapest form of carbonaceous nanomaterials compared to others (e.g. CNTs) (Huang et al. 2014). The most interesting review papers on the manufacturing

of GO and modification are published in the literature (Zhu et al. 2010; Adetayo and Runsewe 2019; Eigler and Hirsch 2014; Agarwal and Zetterlund 2021). The practicality of GO sheets depends on their integration into desired ordered macroscopic materials, such as aerogels (Ji et al. 2013; Qian et al. 2014; Chen and Yan 2011; Tang et al. 2010), hydrogels (Shin et al. 2016; Cong et al. 2013), fibers (Huang et al. 2014; Zhang et al. 2018; Xu et al. 2016b; Wu et al. 2018), and films (Putz et al. 2011; Wang et al. 2018). These materials are associated with superior properties resulting from the attractive inherited properties of graphene (Huang et al. 2014). Thus, they have been employed in different fields, such as wastewater treatment, sensors (Cong et al. 2013), bio-imaging, drug delivery and polymer reinforcement (Putz et al. 2011; Ikram et al. 2020). It is worth mentioning that the self-assembly of GO into ordered structures further broadens the morphology of macroscopic materials in 1D (Huang et al. 2014; Zhang et al. 2018; Xu et al. 2016b; Wu et al. 2018), 2D and 3D (Ji et al. 2013; Chen and Yan 2011; Tang et al. 2010), further expanding the application possibilities of GO. Wang et al. (2018) exploited the synergism of hydrogen bonding and π - π to prepare supramolecular self-assembly of graphene films. The authors prepared 2D graphene multi-layered material by using pyrene (PY) as the source of π - π interaction and

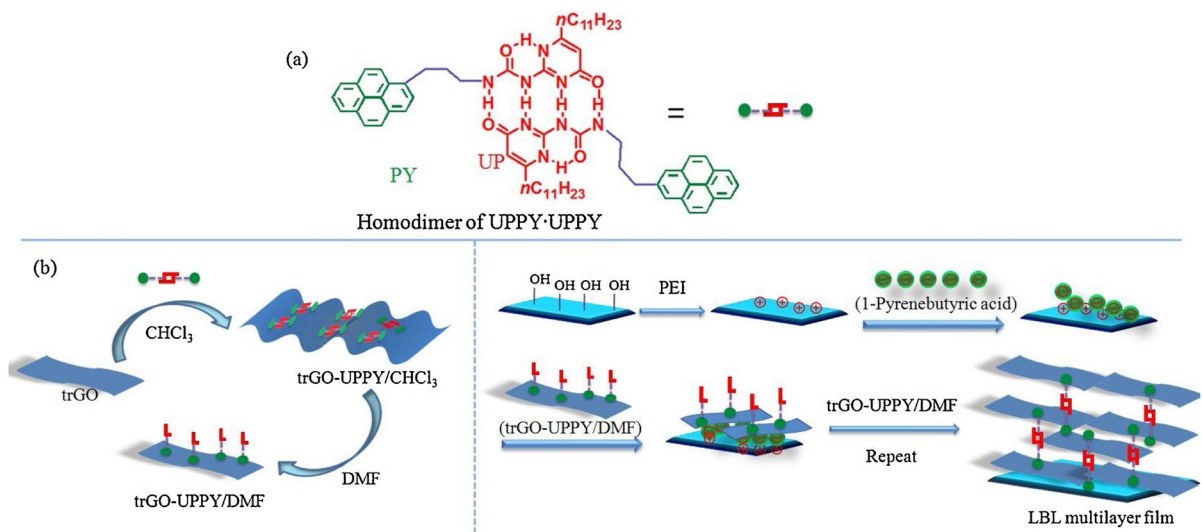


Fig. 2 Schematic presentation of supramolecular self-assembly for fabrication of multi-layered film. Reproduced from (Wang et al. 2018)

Table 2 Properties of carbon-based materials useful for its application

Material	Morphology	Surface area (m ² g ⁻¹)	Diameters (nm)	Lengths (μm)	Density (g cm ⁻³)	Thermal conductivity (W m ⁻¹ K ⁻¹)	Electrical conductivity (S cm ⁻¹)	Tensile strength (GPa)	Modulus (TPa)	Comments	Refs
Graphite	3D	1–132	1500	-	1.9–2.3	25–2000	-	-	0.32–1.02	Cheaper, ease processable and easily accessible	(Tsai and Tu 2010; Zhang et al. 2023)
Graphene	2D	500–2630	6–9	2–2.3	0.77	5000	-	0.0783–130	0.358–1.0 TPa	Ease modification and fairly cheap to produce	(Basu and Bhattacharyya 2012; Lee et al. 2008)
Graphene	3D	850–1628	-	-	~5 mg cm ⁻³	-	10–438	-	-	Ease modification and fairly cheap to produce	(Zhao et al. 2014; Yavari et al. 2011)
CNTs	1D	50–1315	1–10	1–100	0.8–1.8	18.2–70 3000–6600	975–1480	1.77–500	0.97–1.0 TPa	Expensive to produce	(Agarwal and Zetterlund 2021)
Carbon black	3D	10–1443	17–246	-	-	0.3–0.6	-	-	-	Cheaper, and abundant	(Verma et al. 2019)
Carbon nanofibers	1D	20–3000	10–500	0.5–200	1.5–2.0	-	980	-	-	Ease modification and fairly cheap to produce	(Mokhena et al. 2022; Yan et al. 2019)

urediopyrimidinone (UP) for hydrogen bonding, as shown in Fig. 2. These materials exhibit high electron transfer and electrocatalytic performance, and can therefore be used for quantifying dopamine in human fluids (Table 2).

Nanocellulose-graphene hybrid composites

All nanocellulose materials, unless explicitly stated otherwise, will be presented as CNFs throughout the manuscript for the purpose of avoiding misunderstanding. The synergy interaction between 2D GO and 1D CNF is essential for a wide variety of applications (Li et al. 2015). Such interactions are often noticed through improved mechanical performance compared to the resulting materials fabricated from each hybrid components. The most important thing is to achieve a balance between the hybrid components so that they complement each other with their unique properties. CNFs with flexible 1D fibril structure can have good interfacial interactions with 2D GO nanosheets to obtain highly flexible hybrid composites. Physical blending of CNFs suspension with GO powder is the most utilized method to prepare CNFs-GO hybrid composites. This is a cheaper, simple and efficient method to prepare composite materials. In most cases, CNFs can be modified during isolation process to obtain functional groups that improve both the interaction and additional functionalities for the intended applications. Some studies have been carried out to modify already isolated nanocellulose materials to have functionalities that can further improve the interaction with GO. The latter also improves the functionalities for the desired application properties.

The modification of GO can also be employed for the preparation of the desired hybrid composite (Yu et al. 2021). These modification approaches improves the interaction between GO and nanocellulose materials to improve the overall resultant properties. Yu et al. (2021) functionalized GO through an esterification reaction to weaken the hydrogen bonds and chemical inertness. The authors started with carboxylation followed by introducing acyl chloride to produce GO-Cℓ. The resulting GO-Cℓ was combined with nanocellulose material to create a covalent bond between the components of the composite. The resulting layered GO adhered to the surface of the CNFs and formed a rough surface for the composites.

Thermal reduction of GO has also been reported as an alternative method to avoid using chemicals to obtain the reduced GO (rGO) and improve interaction with CNFs (Pottathara et al. 2018).

The preparation of nanocellulose CNF/GO hybrid composites can be achieved using traditional cellulose-based materials preparation methods, such as casting, freeze-drying, and vacuum filtration (Valentini et al. 2013; Liu et al. 2019; Ardekani et al. 2022). These processing methods enable the production of different hybrid composite products, i.e. thin films (Valentini et al. 2013; Ardekani et al. 2022), fibers (Li et al. 2015), aerogels, hydrogels (Zhang et al. 2022), foams (Hao et al. 2022), depending on the desired application. The surface functionality of CNFs plays a critical role in their interaction with GO. GO possess surface functional groups, such as hydroxyl (–OH), carboxyl (–COOH), and epoxy (COC) which make it naturally anionic and hydrophilic. In the case of CNFs, different isolation procedures can significantly change the functional groups. Therefore, the functionalities of both GO and CNFs can be modified to enhance the interaction between these components. For instance, nanocellulose extracted using sulphuric acid introduces additional sulphate groups to the conventional –OH (Valentini et al. 2013). Besides, these functional groups giving the nanocellulose weak anionic character, the resulting mixture with GO improves the dispersion of GO due to electrolytic repulsion between the components. However, the presence of oxygen-containing groups on the GO sheets results in a strong interaction with the –OH groups and the oxygen atoms of the nanocellulose. This leads to hydrogen bonding between CNF and GO, hence improve the structural stability with improved mechanical performance. Furthermore, the properties of these hybrid composites can be tailored through modification of cellulose nanofibrils as their surface functionality controls interfibril interaction. Strong fibril-fibril interaction through hydrogen bonding enhances the mechanical performance of the resulting product because of better stress transfer between the nanofibrils. The modification of GO can also be used to improve the functionality of the product for the desired application. Recent study by Zhang et al. (2022) demonstrated that the mixture of GO and CNFs can be modified using a hydrothermal method for introducing heteroatom-enriched hydrogels for energy storage applications. In this case,

tromethamine was introduced into the mixture as a reducing agent, nitrogen dopant and structural regulator. On the other hand, CNFs served both as a spacer to improve the dispersion of GO and as a reservoir to facilitate the diffusion efficacy of electrolytes within the composite material. The resulting hydrogel exhibited ultra-high gravimetric specific capacitance of $\sim 343 \text{ Fg}^{-1}$ and volumetric, capacitance of $\sim 340 \text{ Fcm}^{-3}$ at 0.3 Ag^{-1} making it good energy storage device. This results from the compactness, abundant heteroatoms functional groups and tuneable porosity. Elsewhere, porous monolith was obtained through urea assisted self-assembly process (Hussain et al. 2018). In their case, Hussain et al. (2018) mixed freeze-dried GO with carbamide salt followed by introduction of CNFs for hydrothermal treatment at 180°C for 5 h. The as-prepared mixture was vacuum freeze dried to obtain porous monolith CNF-GO hybrid composite for dye removal. This demonstrates that the combination of processing methods can be used to manufacture the desired hybrid product for the intended application.

Applications

Cellulose-based composite materials have been widely used in various emerging fields, such as smart portable electronic devices, energy storage/conversion, biomedical, wastewater treatment, air purification, and many others owing to their attractive attributes including remarkable mechanical performance, high thermal stability, low thermal expansion coefficient, tuneable optical properties, and ease functionalization.

Biomedical applications

Natural fibers have gained popularity in biological applications in recent years. Chitosan, collagen, alginate, elastin, gelatin, starch, and cellulose are among natural fibers that have been investigated extensively for biomedical applications (Biswas et al. 2022). Low-cost, renewable, and biodegradable properties are some of the benefits of interest for these types of fibers. It is crucial to note that, in addition to these features, materials for medical applications must fulfill several standards, such as biocompatibility, antimicrobial and antiviral properties to encourage an

optimal host response in a given context. Nanocellulose has received a lot of interest in recent years for its application as a biomedical material due to its exceptional physical features, particularly surface chemistry, and great biological qualities, such as low toxicity, biocompatibility, and biodegradability. This material is commonly used in medical implants, tissue engineering, medication delivery, wound healing, and cardiovascular applications, among other things. Based on the most current scientific research, three main forms of nanocellulose, namely cellulose nanocrystals (CNCs), cellulose nanofibrils (CNFs), and bacterial cellulose (News), are described in terms of their manufacturing techniques, characteristics, and prospective uses. Even though nanocellulose offers unique properties, it lacks antimicrobial and antiviral properties (Neibolts et al. 2020). However, the lack of those properties leads to drug inefficiency which results to mortality and morbidity (Hashem et al. 2022). To address the lack of these properties, Ikram and co-workers in their study developed CNC composite material reinforced with titanium dioxide and GO (Ikram et al. 2022). The introduction of titanium dioxide and GO led to the antimicrobial effect against *E. coli* and *S. aureus*. In addition, the introduction of these fillers into CNC resulted in an improvement in photocatalytic activity against methylene blue, methylene violet, and ciprofloxacin. As mentioned above, to mitigate these shortcomings, functional enhancements, such as fluorescence modification and reinforcement with nanomaterials to improve certain attributes and behaviour are required (Ramani and Sastry 2014). For instance, in a drug delivery system the filler such as graphene is used as a carrier of drugs to make it more efficient (Luo et al. 2017). Nanocellulose composites reinforced with graphene have been a research hotspot. These composites have garnered a considerable interest in biomedical applications such as tissue engineering, drug delivery, biomedical devices, wound healing etc. due to their extraordinary properties.

Tissue engineering

Due to the increasing aging of the population, frequent injuries and chronic diseases, great attention has been paid to the production of scaffolds for tissue engineering from bio-based materials. The ideal scaffolds should replicate the body's extracellular

matrix in terms of properties such as physical structure, biological configuration, and chemical composition (Oprea and Voicu 2020). There have been well-researched studies on the fabrication of tissue engineering from bacterial cellulose (News) (Ramani and Sastry 2014; Oprea and Voicu 2020). This is due to their high purity, biocompatibility, high swelling ability, non-toxicity, purity, abundance, outstanding mechanical properties, and porous structure which is similar to extracellular matrix making them a suitable alternative to petroleum-based materials. In addition, BC does not cause any allergic reaction in comparison to other natural polymers such as collagen and gelatin. This is due to the fact that BC is not originated from animals (Ramani and Sastry 2014; Oprea and Voicu 2020). These unique properties of BC are essential for scaffolds because they permit cellular attachment, cellular migration as well as diffusion of nutrients and metabolites (Oprea and Voicu 2020). In the insightful review reported by Oprea and Voicu (2020), it was highlighted that the scaffolds made from BC improve the rate of tissue regeneration while reduces the inflammatory response.

Despite the outstanding properties of BC, there are limitations when virgin cellulosic materials are employed to fabricate scaffolds for tissue engineering. One of the major limitations is the insufficiency of bioactivity and electrical conductivity properties which limits their applications, especially in bone tissue engineering. Also, although BC have good mechanical- properties, their mechanical properties do not match well with those of natural bone tissues (Wahid et al. 2021). One of the mitigation factors to address these limitations is incorporating fillers to improve bioactivity and mechanical properties. Hydroxyapatite is a well-researched filler used in bone tissue engineering. This filler enhances osteoblast compatibility, and osteoprogenitor attachment and promotes new bone formation (Ramani and Sastry 2014; Niamsap et al. 2019; Cao et al. 2022). For instance, Niamsap et al. (2019) fabricated hybrid BC-based scaffolds reinforced with hydroxyapatite and CNC for bone tissue engineering. The results demonstrated that the hybrid material improved thermal stability. In addition, cytotoxicity (MTT assay) results revealed that the hybrid material had cell viability of $83.4 \pm 3.6\%$ which was above the cell viability threshold of 70% for cytotoxicity analysis. These results suggested that the resultant hybrid material was not

harmful to cell growth. However, the resultant hybrid material had the potential to regenerate damaged tissues and promote the formation of new tissues (Khan et al. 2022). In another study by Ramani and Sastry (2014), BC was reinforced with two inorganic fillers (hydroxyapatite and GO). The results showed that the resultant composite material promotes the adhesion of osteoblast cells with good cell viability. The osteoinductive potential as well as the biocompatibility of the resultant scaffolds was investigated. It was revealed that the scaffolds demonstrated biocompatibility on MG-63 and NIH 3T3 cell lines. In addition, the alkaline phosphatase activity assay using MG-63 cells showed that the scaffolds have the potential to be osteoinductive material in *in-vitro* (Hwang et al. 2024).

In recent years, there has been an increasing demand to fabricate scaffolds with electrical conductivity properties while maintaining other properties such as biocompatibility, non-toxicity, and outstanding mechanical properties (Jin et al. 2016; Chen et al. 2016a). Graphene and GO have attracted research interest in biomedical applications due to their electrical conductivity properties together with outstanding mechanical, optical, large surface area as well as tailorable surface properties (Jin et al. 2016; Chen et al. 2016a; Luo et al. 2019a; Azarniya et al. 2016; Torres et al. 2019). Even though GO displayed unique properties, the processes of fabricating GO results in the material comprises of significant increased surface hydrophobicity while improving electrical conductivity properties. This limits their applications in biomedical applications due to incompatibility to support cell adhesion and growth (Jin et al. 2016). Incorporation of graphene-based materials into BC is considered a suitable approach to develop scaffolds with electrical conductivity properties and compatibility with cells while maintaining other properties. Numerous researchers fabricated BC composite materials reinforced with graphene with improved mechanical and electrical conductivity properties for biomedical applications (Azarniya et al. 2016; Torres et al. 2019; Luo et al. 2019b, 2018; Guan et al. 2019; Si et al. 2014; Rashidian et al. 2021). For instance, in the study reported by (Luo et al. 2019b), BC reinforced with graphene was prepared by cycled film-liquid interface culture (CFLIC) and hot-pressing method. The cross-sectional surface area demonstrated that graphene was well dispersed in BC. Contact angle

increased upon addition of graphene indicating that the hydrophobicity of the material was increasing. Additionally, the incorporation of graphene up to 2% improved thermal stability, tensile strength, tensile modulus, and strain at break as well as electrical conductivity properties. It is worth noting that biocompatibility of the resultant composite materials was not investigated in most of these studies.

There are very few studies investigating biocompatibility between BC-based materials reinforced with GO and cells. Among those studies, (Jin et al. 2016), (Chuntao Chen et al. 2016a), (Luo et al. 2019a), and (Shende and Pathan 2021) have reported the biocompatibility between BC graphene-based materials and cells. Highly biocompatible with electroactivity materials were prepared from BC, poly(3,4-ethylene dioxythiophene), and GO by in-situ polymerization (Chen et al. 2016a). The mechanical properties of the prepared films were comparable to natural collagen protein. The cytotoxicity assessment of prepared films using MTT cell viability assay revealed that the prepared films exhibited very low cytotoxicity for PC12 neural cells. These results suggest that the prepared films demonstrated good biocompatibility with PC12 neural cells due to the adhesion of the cells. In addition, the cells grew well on the prepared films. Similarly, Luo et al. (2019a) and Jin et al. (2016) prepared films from bacterial cellulose and GO with excellent mechanical and electrical conductive properties. In the case of Luo et al. (2019a) the prepared films demonstrated good biocompatibility, cell adhesion, spreading, and proliferation as well as good osteogenic differentiation with mouse embryo osteoblast (MC3T3-E1) cells. In the study reported by Jin and co-workers human marrow mesenchymal stem cells (hMSCs) were used to evaluate biocompatibility with films prepared from BC and GO (Jin et al. 2016). The results demonstrated that the films exhibited better cellular response and adhesion with improved cell proliferation. It can be concluded that the BC-based films are biocompatible and can provide a good environment for the PC12, MC3T3-E1, and hMSCs cell growth and proliferation. Therefore, these materials are regarded as suitable candidates for tissue engineering.

Even though BC reinforced with GO is well-researched and showed potential for tissue engineering. There are few studies reported in the literature on the composites developed from CNC and CNF

reinforced with GO for tissue engineering. It is worth noting that CNC requires carrier material in the form of a polymeric matrix, unlike BC. This could be due to their brittle behavior. Various polymers such as polylactic acid (Neibolts et al. 2020; Pal et al. 2017, 2019a), collagen and gelatin (Salleh et al. 2022), and polybutylene succinate (PBS) (Neibolts et al. 2020). The introduction of CNC and GO into PLA hybrid material improved their mechanical, thermal, and antimicrobial properties. In addition, the developed hybrid materials displayed good biocompatibility with fibroblast cells such as C3H10T1/2, NIH-3T3) and epithelial cell line HEK293T. The cells remained healthy after 7 days of incubation indicating that the developed hybrid materials are non-toxic in cells (Pal et al. 2017, 2019b). Therefore, due to the outstanding properties of developed hybrid materials, they can be utilized as scaffolds in tissue engineering. A similar trend was observed when natural polymers such as gelatin and collagen were employed (Salleh et al. 2022). In another study, electrospun fibres were fabricated from PBS, CNF, and graphene nanoplatelets as scaffolds for tissue engineering (Neibolts et al. 2020). Fourier-transform infrared (FTIR) and Raman spectroscopy suggest that there was a good interaction between fillers and polymer matrix. The electrospun fibres developed had high quality indicating that they are suitable for tissue engineering as scaffolds. Further research on electrospun fibres to determine their biocompatibility, cytotoxicity, cell attachment, growth, and proliferation should be undertaken.

Wound healing

Wound treatment has been the major challenge and there is a growing demand for the development of biomaterials to accelerate wound healing. Wound dressing is one of the strategies to accelerate accelerating wound healing. According to Grand View research, the market of wound dressing has a huge market globally. The market was valued at \$7.4 billion by 2022, and it was anticipated to expand at a compound annual growth rate (CAGR) of 4.5% from 2023 to 2030 (https://www.marketsandmarkets.com/Market-Reports/advanced-wound-care-market-88705076.html?gclid=CjwKCAjwhdWkBhBZEiWAl1bLmATvSIR1M5MFGzW_Z9wrcndx-uYWuQqPuNjNq4wh1uUbc018aeOorhoCcb4QAvD_BwE, Accessed on 15 December 2023). The growth of this

market is influenced by several factors such as an increase in road accidents, chronic wounds such as diabetes, cancer, burn injuries, and surgical procedures. The wound dressing products comprise foam dressing, film dressing, and others. Therefore, the development of wound dressing from eco-friendly materials will play an imperative role in the wound care industry. These materials can be directly applied to the wound (primary wound dressing) or on top of the primary dressing (secondary wound dressing) (Zmejkoski et al. 2022). The ideal wound dressing should be able to remove exudate, inhibit bacterial growth, be non-toxic, biocompatible, provide a moisture atmosphere, low allergic reaction, and have good permeability properties as well as inhibiting dressing peeling off with the skin (Zmejkoski et al. 2022).

Nanocellulose possesses many intrinsic properties as mentioned in the following section that can accelerate the healing of the wound (Portela et al. 2019). Novel hydrogels fabricated from BC reinforced with graphene quantum dots demonstrated good antimicrobial properties against *S. Aureus*, *S. Agalactiae*, *E. Coli*, and *P. Aeruginosa*. The healing process was conducted using *In-vitro* analysis on human fibroblasts. It was observed that there was a significant migration of human cells after the application of the resultant hydrogels, thus improving angiogenesis. Furthermore, the fabricated hydrogels exhibited good wound fluid absorption as well as water retention. These properties suggest that the developed hydrogels are suitable to be used as wound dressing (Zmejkoski et al. 2022). In another study, it was reported that the incorporation of GO into hydrogels bacterial nanocellulose (BNC)-grafted poly(acrylic acid) (AA) enhances water vapour transmission rates, decreases hardness and bio-adhesion while improving durability and easily removable properties which is the requirement for an ideal wound dressing material (Chen et al. 2019). Moreover, the hydrogels displayed good biocompatibility making them a suitable candidate for wound dressing. This trend was also reported in other studies (Salleh et al. 2022; Khan et al. 2023). The hydrogels prepared from CNC, chitosan and GO displayed higher water absorption capacity and water retention capacity. It was also observed that hydrogels showed low cytotoxicity against 3T3 fibroblasts and antimicrobial properties against *E. Coli*, *S. Aureus*, and *C. Albicans* (Yang et al. 2019).

Other researchers proposed the development of a transdermal patch from bacterial cellulose (Khamrai et al. 2019). In their novel patch, they incorporated dopamine to provide mussel mimetic properties and silver nanoparticles as well as GO to provide antimicrobial against *S. Aureus*, *L. Fusiformis*, *E. Coli*, and *P. Aeruginosa*. In addition, the incorporation of GO facilitated wound healing properties as well as electrical conductivity properties. The *In-vitro* analysis on NIH 3T3 fibroblast and A549 human lung epithelial cells suggests that the incorporation of nanofillers accelerates the wound healing process. Similar behaviour was observed in another study reported by (Zhang et al. 2021).

Mechanical properties play a pivotal role in developing materials for wound dressing. Electrospun 3D porous mat from BC and chitosan blends have shown a potential for wound dressing (Azarniya et al. 2016). However, their mechanical structure may not be adequate and compatible with natural skin tissue. To strengthen the mechanical properties of the mats, GO was incorporated. In addition, the incorporation of GO reduced the water vapour permeability making them suitable for wound dressing.

Nanofibres from cellulose acetate (CA) reinforced with GO and other nanofillers were fabricated using electrospinning (Kim and Park 2022; Prakash et al. 2021) and hydrogels (Aly and Ahmed 2021) for wound healing applications. The addition of GO and other nanofillers such as titanium dioxide and zinc dioxide into CA nanofibres enhanced their mechanical and antimicrobial properties against wound pathogens. The cell viability displayed progression of about 97% and the human fibroblast cell attachment in nanofibrous materials suggests that cells were proliferated and spreading through the material. In addition, curcumin was added to CA nanofibers. The results demonstrated that sustained curcumin release enhances skin regeneration and wound healing. This active wound dressing was also prepared from BC and GO (Gabryś et al. 2022; Al-Arjan et al. 2022). The active wound dressing from BC was aimed at releasing paracetamol and curcumin. The paracetamol release rate was achieved at 80% after 24 h (Gabryś et al. 2022). In the case of curcumin, the drug release rate is depicted in Fig. 3 at 7.4 pH. It was observed that after 33 h, the release rate of curcumin

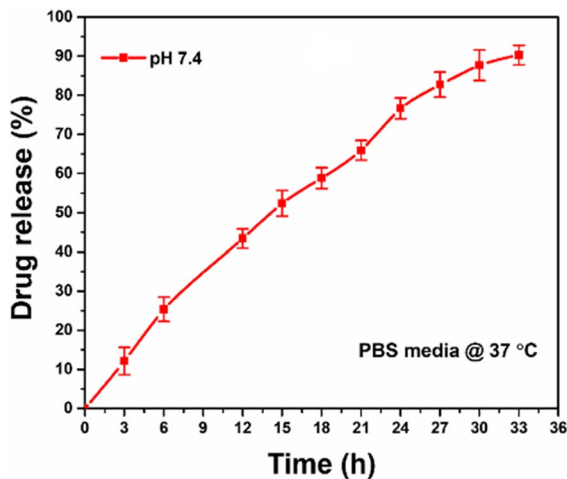


Fig. 3 The drug release of curcumin at 37 °C under pH 7 (Al-Arjan et al. 2022). Open access

achieved about 91%. In addition, the developed material displayed antimicrobial properties against *S. aureus*, *E. coli*, and *P. aeruginosa* as well as anticancer activities (Al-Arjan et al. 2022).

Other medical applications

Currently, nanocellulose and graphene oxide-based materials have been widely used in tissue engineering, and wound healing applications such as wound dressing. As above mentioned, these materials are widely used due to their unique properties. Although nanocellulose and graphene oxide-based materials have been explored in those applications, there is limited research conducted on other biomedical applications such as drug delivery, biomedical devices, and smart sensors. Also, there are few commercially available products from nanocellulose and GO for biomedical applications. Since the production of nanocellulose is growing and the fact that nanocellulose can be tailored to improve the properties of the intended applications, there will be numerous applications of nanocellulose-based products for biomedical applications in the near future. For instance, there is a potential for developing 3D printed biomedical devices from nanocellulose and GO-based materials as a suitable replacement for petroleum-based products.

Several factors led to less exposure to nanocellulose and graphene oxide-based materials for biomedical applications. One of the factors is the market is still in

the infancy stage and the production of nanocellulose is not well established in comparison to petroleum-based products. Secondly, clinical studies are limited to in vitro and in vivo using cell lines and animal models to determine their biocompatibility (Portela et al. 2019). However, according to our best understanding, there are very few or no studies conducted on human trials. Bacterial cellulose has been widely explored because of its purity. However, there is a lack of research work on other nanocellulose i.e. CNF and CNC. Therefore, much research is required to explore and exploit CNF and CNC in various biomedical applications. Different studies on various biomedical applications such as drug delivery and medical devices from nanocellulose-based GO materials are listed in Table 3 (Wang et al. 2023; Kim et al. 2015; Zhu et al. 2015; Urbina et al. 2020; Stanisic et al. 2022; Passornraprasit et al. 2022; Shi et al. 2023).

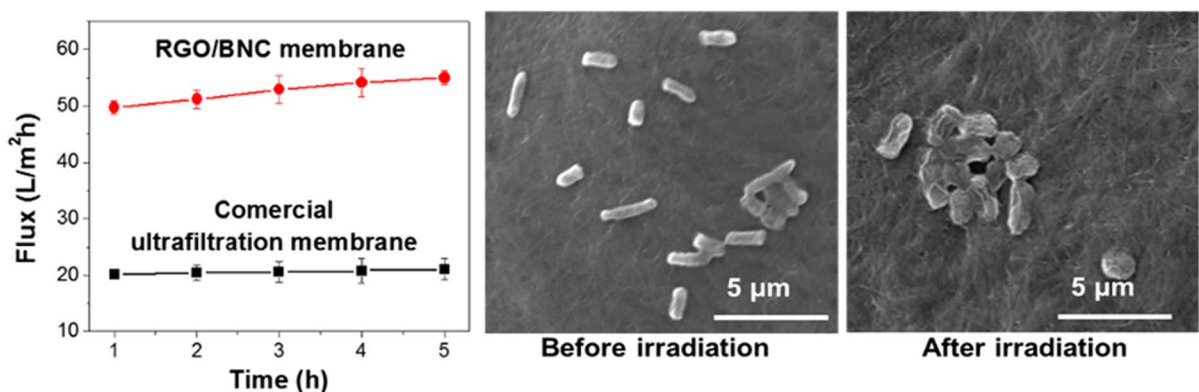
Wastewater treatment

Membrane filtration

A wide variety of technologies have been employed for the purification of polluted water, such as membrane filtration, solar evaporation, reverse osmosis, etc. Filtering membranes are commonly employed for the removal of pollutants through a size exclusion mechanism. This means that the membrane efficiency or performance relies on selectivity, flux, durability, and low energy consumption (Xu et al. 2018; Mokhena and Luyt 2017; Mokhena et al. 2022). The membranes composed of cellulose/GO have been developed to purify water because of their superior chemical stability, high purification efficiency, no or less environmental impact, and ease of preparation (Jiang et al. 2019). In most cases, the selectivity of these membranes is often improved by chemical modification and/or the inclusion of additional functional materials. These functionalities can further provide other essential aspects to the membrane to enhance the overall purification efficiency (Jiang et al. 2019). The incorporation of reduced GO into bacterial CNFs resulted in an ultrafiltration membrane with superior mechanical and chemical stability under different pH conditions and strong agitation. The membrane exhibited excellent water flux under high pressures with light-enabled bacterial activity towards *E. coli*, as shown in Fig. 4. The antibacterial efficacy was enhanced by the remarkable photothermal property of the membrane.

Table 3 Other applications of nanocellulose and graphene-based materials

Materials	Intended applications	Remarks	Reference
BC/GO	Drug delivery	- FTIR reveal interaction between BC and GO - Successfully release ibuprofen (IBU)	(Luo et al. 2017)
Polydopamine/CNF/GO hydrogels	Drug delivery	- Displayed high drug loading (up to 35%) - Improved mechanical properties - Successfully release drug - Low cytotoxicity	(Liu et al. 2020)
BC/GO	Drug delivery	- Good interaction between materials - Good biocompatibility and facilitate cell proliferation	(Zhu et al. 2015)
BC/GO hydrogels	Drug delivery	- Promotes ibuprofen (IB) release	(Urbina et al. 2020)
CNF/Silver nanoparticles/GO	Nasal, mouth, and eye spray	- The composites displayed high virucidal properties and inhibited the viral activity in cells - The material displayed low toxicity in cells	(Stanisic et al. 2022)
BC/GO	Wearable and implantable electronic devices	- Better wettability and mechanical properties - Good biocompatibility - Excellent electrochemical properties	(Guan et al. 2019)
CNF/GO/polyacrylic acid hydrogel	Sensing patch	- Enhanced mechanical properties - Improved laser desorption ionization of urea and functionalities	(Passornraprasit et al. 2022)
Oxidized BC/GO hydrogel	Biomimetic nerve grafts	- Improved stiffness - Facilitate the development of growth cones and filopodia	(Shi et al. 2023)

**Fig. 4** Water permeation of rGO/BNC membranes and commercial ultrafiltration membrane at 100 psi and SEM images of *E. coli* on the membrane before and after irradiation. Reproduced from (Jiang et al. 2019)

Catalysis

Catalysts have been used to degrade pollutants as a suitable solution for wastewater treatment (Hao et al. 2022; Qiu et al. 2022; Fan et al. 2015; Lefatshe et al. 2017; Anirudhan et al. 2016). A wide variety of fillers with catalytic properties can be used to decorate CNFs and GO (Lefatshe et al. 2017; Anirudhan et al. 2016; Roy et al. 2023). There has been minimal investigation into the application of CNF/GO hybrid composites for catalyzing the breakdown of diverse water contaminants (Table 4) (Hao et al. 2022; Anirudhan and Deepa 2017). In general, the catalytic activity of the CNF/GO hybrid mostly depends on additional filler incorporated into the system since both CNFs and GO have no catalytic properties. However, the synergy between CNF/GO which facilitates electron conductivity and hydrophilicity with the secondary filler has been reported to improve the overall catalytic efficiency of the GO/CNF hybrid (Hao et al. 2022; Anirudhan and Deepa 2017). It is noteworthy mentioning that this provides an opportunity for further research on the use of CNF/GO hybrid composites in catalytic degradation of the pollutants from wastewater. The hybridization of these materials promises to offer composites with enhanced properties indicative of the individual properties exhibited by each constituent decorated with catalytic fillers.

The new possibility of degrading metalloids received considerable attention from researchers due to the results obtained from changing Cr(IV) to Cr(III) via photodegradation process (Hao et al. 2022; Fan et al. 2015). This development is essential for the removal of toxic metalloids from strained water resources (Hao et al. 2022; Fan et al. 2015). CNF/GO/graphitic carbon nitride (g-C₃N₄) foam was prepared

via self-assembly for photodegradation of Cr⁶⁺ to Cr³⁺ (Hao et al. 2022). The high affinity between g-C₃N₄ and CNFs resulting from electrostatics and crosslinking with GO serving as a binder strengthened the hierarchical porous foam (Fig. 5a-b). The resulting foam showed excellent flexibility and stability over 50 compressive cycles (Fig. 5c). It exhibited a high specific area of 135 cm³g⁻¹, porosity of 95.9%, and density of 29 mg cm⁻³ with remarkable tolerance to acidic and alkaline conditions. It was used as a catalyst with the aid of visible light. The photocatalytic activity increased with an increase in g-C₃N₄ content due to its abundant available active sites (Fig. 5d-e). The optimal content of 60wt% exhibited a reduction capacity of 98% with a slight decline in photocatalytic activity after 9 regeneration cycles (Fig. 5f). This indicates that the resulting hybrid was stable and maintained its original microstructure and morphology upon regeneration. The strong interaction between CNF and GO as a base accommodated g-C₃N₄ to maintain a high surface area for exposure of active sites to afford high photodegradation efficiency. The primary mechanism involved irradiation of hybrid lead to excitation of g-C₃N₄ to generate photo-induced electrons and holes with hierarchal porous structure affording efficient charge transport (Fig. 5g). CNFs with inherently hydrophilic character promotes active species transfer in aqueous medium with GO serving as electron collector due to its excellent electron conductivity. The resulting electrons migrate to Cr(IV) species to prevent the recombination of electrons and holes. In addition, GO facilitates the overall conductivity of the hybrid to maintain the separation of electrons and holes.

A porous GO/CNC/ZnO hybrid synthesized as a catalyst for the degradation of ciprofloxacin (CF) was demonstrated by Anirudhan and Deepa (2017). The inclusion of ZnO in GO increased from the band gap

Table 4 Summary of studies on decontamination of water using CNF/GO hybrid composites

Materials	Form	Pollutant	Efficiency (%)	Time (min)	Light	Regeneration cycles	Refs
CNF/GO/g-C ₃ N ₄	Foam	Chromium	98.0	180	Sunlight	9	(Hao et al. 2022)
CNF/GO/ZnO	Membrane	Ciprofloxacin	98.0	40	Sunlight	5	(Anirudhan and Deepa 2017)
CNF/GO/Pd	Membrane	Methylene orange	100	5	-	10	(Xu et al. 2018)
CNC/GO-doped TiO ₂ quantum dots	-	MB, methylene violet, ciprofloxacin	95.5	-	Mercury light	-	(Ikram et al. 2022)

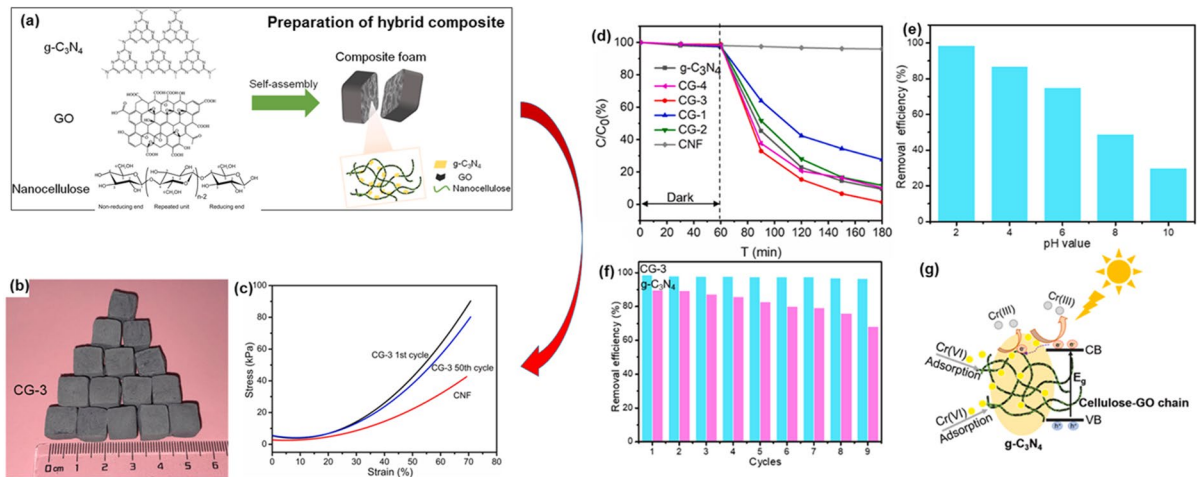


Fig. 5 (a) Preparation of a CNF/GO/g-C3N4 hybrid through self-assembly to create flexible porous foam. (b) Image of the resulting porous foams, and (c) compressive stress-strain curves of CNF and the porous foams. (d) Photocatalytic performance of the prepared samples, (e) reduction of Cr(VI) at

different pH levels, (f) cyclic testing of the porous foam and g-C3N4 powder. (g) The proposed mechanism for the photocatalytic reduction of Cr(VI) over the porous foam. Reprinted with permission from (Hao et al. 2022). Inserted glucose unit in (a) is reproduced with permission from (French 2017)

from 2.4 eV to 2.8 eV within the visible region making the hybrid desirable for photodegradation of CF. The as-prepared hybrid exhibited a surface area of $13 \text{ m}^2 \text{ g}^{-1}$, pore volume of 0.026 mL g^{-1} , and pore radius of 12.5 nm. The degradation efficiency of $\sim 98\%$ was attained within 40 min at a pH value of 6. The primary mechanism involved the irradiation of the hybrid with photon energy higher than its band gap to afford the generation of valence band electrons and conduction holes. The resulting charges are then moving onto the surface during the degradation process, meanwhile, excitation of CF affords it the opportunity to act as a light sensitizer and electron acceptor. Therefore, excited CF can be adsorbed on the surface of the hybrid to afford its degradation to non-toxic products. The regeneration over 5 cycles resulted in degradation capacity decreasing from 98% to 84.3% which indicates the hybrid can be used for practical purposes. The additional functionality from palladium nanoparticles (PdNPs) into CNF/GO composite membrane afforded excellent photocatalytic properties as reported for the first time by (Xu et al. 2018). PdNPs were in situ grown within GO/CNF aerogel obtained from the freeze drying process through the introduction of Pd precursor into the porous structure to a highly uniform distributed PdNPs loaded membrane. The catalytic activity was established using

methylene orange (MO) as a model dye in the presence of NaBH_4 . The immersion of the membrane into the dye solution resulted in the complete disappearance of the intense absorption peak at 465 nm, indicating complete degradation of the dye sample. The immersion of CNFs and CNF/GO without PdNPs, however, resulted in an absorption peak at 465 nm remaining virtually the same after 5 min. The latter indicates that both GO and CNFs have no catalytic activity but the inclusion of the nanofillers is necessary to degrade pollutants. The authors also studied the importance of using GO as a template for the in situ synthesis of Pd nanoparticles by in situ growing PdNPs onto CNFs alone. They found that the rate of degradation was lower when compared to that of samples made from in situ growth of PdNPs in CNF/GO aerogel. For regeneration and reusability, CNF/GO/PdNPs hybrid composite was washed with water/ethanol. Hybrid composite maintained high catalytic activity even after 10 cycles and retained $\sim 95\%$.

Besides, GO being an excellent substrate material for the synthesis of NPs because of its attractive features, such as high thermal stability, chemical stability, desirable functionalities, and large surface area, the poor stability in aqueous solution, and limited mechanical performance hurdle its widespread application in pollutants degradation settings. Therefore, combination with

CNFs serves as the ideal approach to manufacturing hybrid composites with acceptable mechanical performance and large surface with good stability in an aqueous medium. In addition, CNFs promote the dispersion of GO composites through intercalation to afford richly functional materials with mechanical robustness, excellent catalytic stability, and reusability.

Dye removal

CNF/GO hybrids have been explored for the removal of dye from coloured wastewater streams, as reviewed in Table 5 (Wei et al. 2019; Liu et al. 2019; Dogra et al. 2022; Walling et al. 2023). Xu et al. (2018) investigated the influence of PdNPs on the dye

Table 5 The use of GO/Cellulose hybrid composites for dye removal

Sample	Surface modification	Form	Mechanism	Contaminant	Efficiency (%)	Time (Minutes)	Capacity (mg g ⁻¹)	Cycle number	Refs
Tempo-oxidized CNF/GO	TEMPO oxidized CNFs	Monolith	Adsorption	MB	100	150	227	4	(Hussain et al. 2018)
CNF/GO	-	Aerogel	Filtration	MB	-	-	266	-	(Wei et al. 2019)
				CR	-	-	22	-	(Liu et al. 2019)
				VBB	99	-	-	-	(Liu et al. 2019)
				MV2	98	-	-	-	
				R6G	92	-	-	-	
CNF/GO	-	Aerogel	Adsorption	MB	-	250	112.2	3	(Wang et al. 2021b)
				Tetracycline	-	250	47.3	-	
CNF/GO	-	Aerogel	Adsorption	MB	99	20	10.48	6	(Nguyen et al. 2022)
CNF/GO	TEMPO oxidized CNFs	Aerogel	Adsorption	MB	98	100	588.23	4	(Abouzeid et al. 2022)
CNF/GO/SiO ₂							625		
CNC/GO	H ₂ SO ₄ hydrolysis	Membrane	Dynamic fixed bed	BB7	100	1170	213	3	(da Silva et al. 2021)
			Adsorption	MO	-	-	681.82	-	
			Adsorption	Reactive orange 122	-	-	9.18	-	
CNF/GO/MWC-NTs-NH ₂	Amine functionalized	Aerogel	Adsorption	Sesame	100	20a	124	-	(Hui et al. 2021)
				Ethyl acetate	-	-	162	-	
				Dichloromethane	-	-	154	-	
				Cyclohexane	-	-	93	-	
				Acetone	-	-	104	-	
CNF/GO	-	Aerogel	Adsorption	Pump oil	-	-	26	-	(Wei et al. 2019)

a=seconds

removal efficiency of CNF/GO aerogel. It was demonstrated that the membrane can completely remove MO from orange-coloured water. It was reported that the membrane maintained high dye removal efficiency (> 99%) up to 60 mg L⁻¹ of dye concentration, with a slight reduction at 80 mg L⁻¹ to ~90.5%. In addition, the membrane showed excellent degradation efficiency under different pH conditions (pH 3–9) with good regeneration stability by retaining more than 99% of its initial degradation after 6 cycles. Using a cocktail of (50 mL) contaminants (rhodamine 6G (R6G), methylene blue (MB), and 4-nitrophenol (4-NP), each with a concentration of 10 mg L⁻¹), it was noticed that the membrane effectively removed all these pollutants. The membrane was capable of removing particles sized ~5 nm, meanwhile maintaining a high permeation of 33.1 L m⁻² h⁻¹ over 6 h at a pressure of 58 psi, i.e. 2.3 and 2.8 times higher than commercially available nanofiltration membranes, due to a tortuous network of pores within the composite membrane resulting from all the components.

Cellulose nanocrystals (CNCs)/GO nanocomposite was reported for dye adsorption (da Silva et al. 2021). GO was obtained through the modified Hummers method which resulted in oxidized and exfoliated nanosheets with a width of ~0.52 and thickness

of ~1.5 nm bearing oxygenated groups to afford strong interaction with CNCs, needle-shaped particles with a width of ~220 nm and thickness of ~5 nm, through hydrogen bonds (i.e., CNCs' -OH and GO' -OH/ -COOH groups) and p- π interactions from -OH from CNCs and π electrons from GO aromatic ring (Fig. 6a). The resulting composite with large surface area, and a large number of -OH, -SO₃ and -COOH functionalities as well as aromatic rings making it favourable to form coordination with complex aromatic dyes. The as-prepared composite was applied for the adsorption of dyes (basic blue 7 (BB7), reactive orange 122 (RO), and rhodamine B (RhB), from coloured wastewater samples (Fig. 6e). All composites showed high adsorption capacity for different dyes, but CNC/GO 70/30 displayed superior adsorption efficiency with instantaneous BB7 adsorption capacity of 1943 mg g⁻¹ when BB7 concentration is 100 mg L⁻¹ and adsorbent dosage is 0.1 g L⁻¹ at 298 K and pH value 6 (Fig. 6d). The increase in temperature gradual decreased the BB7 removal efficiency of the composites, i.e. from 891 mg g⁻¹ (87%) to 617 mg g⁻¹ (63%) when the temperature is increased from 298 to 328 K (0.1 g L⁻¹ adsorbent dosage, BB7 concentration of 100 mg L⁻¹, sonication for 2 min, pH value of 6). The main concern was

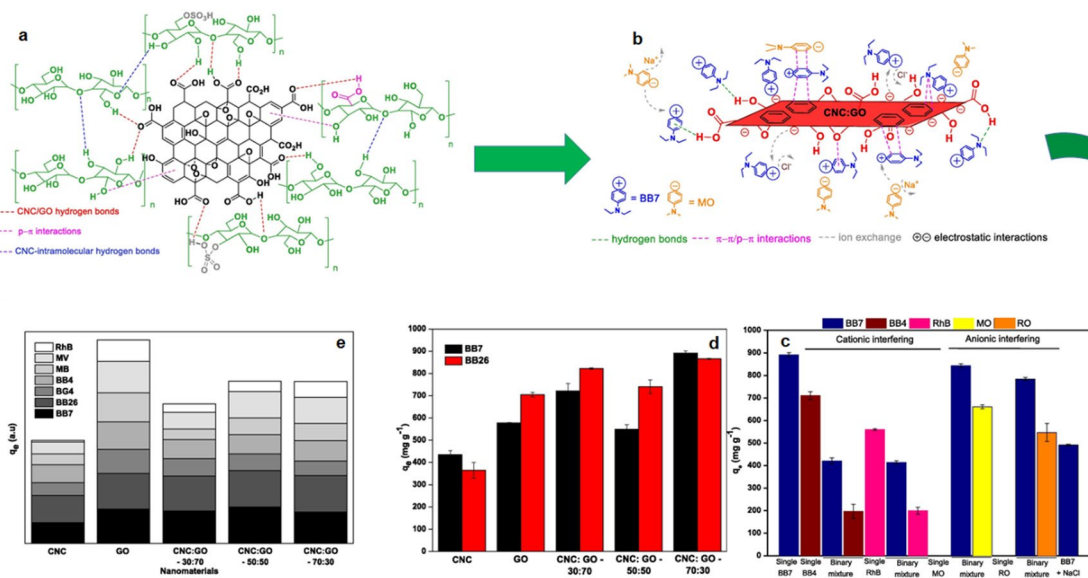


Fig. 6 **a** The interaction between CNCs and GO in resulting composite material, **(b)** proposed interaction mechanism of the dyes with CNC/GO composite, and **(e-d)** adsorption behaviour

of CNC/GO for different dyes. Reprinted with permission from ref. (da Silva et al. 2021). Copyright 2021 Elsevier

the recyclability of the composite with q_e decreasing from 989 mg g⁻¹ to 313 mg g⁻¹ and 242 mg g⁻¹ for the second and third sorption–desorption cycles, respectively. Nonetheless, the composite exhibited 77% BB7 removal efficiency within 120 min from the river, while high selectivity for BB7 in the binary dye solution. In a binary mixture of BB7 with MO and RO led to the adsorption capacity of 681 and 516, respectively because of a synergistic effect (Fig. 6c).

Three-dimensional (3D) aerogel composed of CNFs and GO has been explored as feasible and effective adsorbents membranes for the removal of various pollutants from wastewater streams (Al-Shemy et al. 2022; Gu et al. 2021; Wang et al. 2021b; Nguyen et al. 2022). In this case, the mixture of cellulose/GO suspension is frozen and then freeze-dried to afford adsorbents with high porosity, large surface area, and excellent adsorption capacity. The resultant aerogel is usually ultralightweight with remarkable compressive strength. A recent study by Nguyen et al. (2022) demonstrated that 13wt% of GO into CNFs is a sufficient content to fabricate aerogel with superior adsorption efficiency of 99% within 10 min, as shown in Fig. 6a. The aerogel composite removed more than 99% after 90 min, whereas pure CNF and GO removed ~95% and ~64%, indicating that combination of GO and CNFs significantly enhance MB removal efficiency (Fig. 7a). In addition, the aerogel composite was more durable and stable in aqueous medium when compared to GO and CNF-based aerogels with debris settling at bottom of the cuvettes being observed after 90 min (Fig. 7b). CNF/GO aerogel was more resilience for five sorption–desorption cycles with ~2% decrease per sorption–desorption cycle, but drastically decreased to 6% after 6 cycles (Fig. 7c and d). The strong electrostatic interaction between MB and CNF/GO aerogel, and structural integrity due to the reinforcing effect of GO and GO as an electron acceptor via π - π stacking for MB-saturated double bonds were the main contributors to such excellent performance. Moreover, the MB/methyl orange (MO) selectivity of CNF/GO aerogel was remarkable within 20 min due to its strong affinity for cationic dyes.

Hussain et al. (2018) fabricated a monolith from TEMPO-oxidized CNFs in the presence of GO. The mixture of GO and CNFs in the presence of

carbamide salt was freeze-dried after hydrothermal treatment to obtain a highly porous monolith with dye adsorption capacity of 151–227 mg g⁻¹. The results were ascribed to the increase in CNF content which afforded changes in the structure accompanied by additional functionalities brought by oxidized CNFs. The increase in CNFs content increases the specific surface area on the hybrid composites leading to an increase in dye adsorption efficiency.

The inclusion of other materials into the CNF/GO composite can further improve the adsorption rate and capacity of the resulting aerogel (Sajab et al. 2016). The introduction of iron chloride into GO and then added into CNFs resulted in rapid adsorption of 10 min and reached maximum adsorption of 142.3 mg g⁻¹. The as-prepared composite showed a decline in adsorption efficiency after the 3 sorption-oxidation process. In their work Al-Shemy et al. (2022) prepared aerogel composed of alginate, cellulose, and GO for methylene blue removal. 10% of cellulose particles within the composites exhibited excellent dye removal efficiency due to low density, higher surface area, and good compressive strength. The incorporation of silica using TEOS precursor into GO/CNFs aerogel resulted in superior MB adsorption when compared to GO/CNFs composite over the investigated pH values (Abouzeid et al. 2022). Adsorption capacities increased with an increase in pH for both CNF/GO and CNF/GO/SiO₂ composites reaching 85 and 95 mg g⁻¹ at neutral pH because of the deprotonation of surface functional groups to draw more MB molecules. The presence of silica significantly improved the MB adsorption capacity of the composite deduced using the Langmuir model from 588 mg g⁻¹ (CNF/GO) to 625 mg g⁻¹ (CNF/GO/SiO₂).

Oil removal

Oil spills and organic solvent pollution from various industries are the major water pollutants and can cause drastic to the environment, and people's health (Wan and Li 2016). Different technologies have been developed in order to treat the oily wastewater. The use of adsorbents has been considered one of the most efficient and simple methods for oily water treatment. A wide variety of adsorbents (e.g., activated carbon, bentonite, fly ash, hybrid materials) have been used

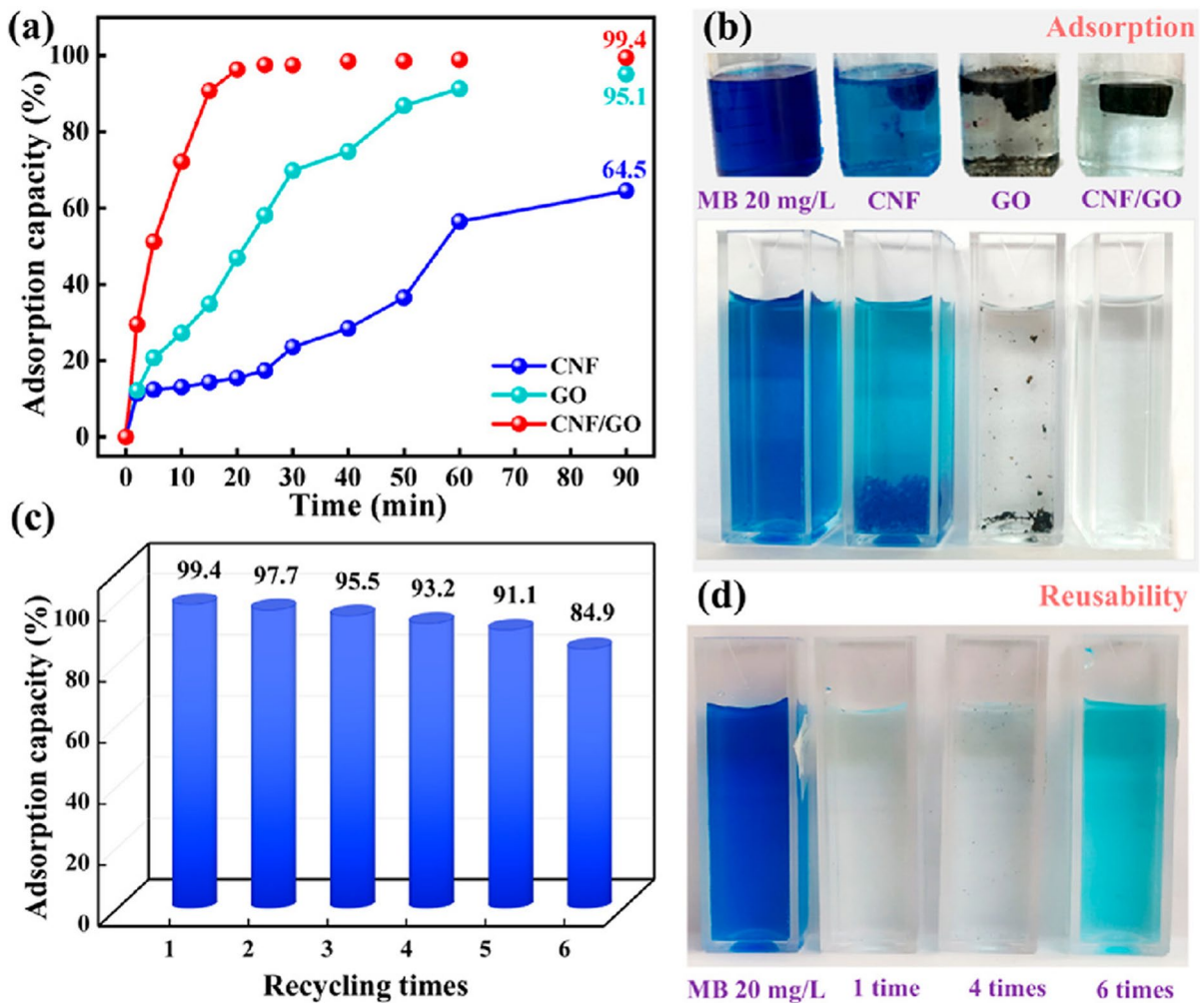


Fig. 7 a Removal efficiency, (b) resultant MB solution after adsorption for 90 min onto GO, CNF, and CNF/GO aerogel, (c) regeneration of CNF/GO aerogel, (d) MB solutions after

1, 4, and 6 sorption–desorption cycles onto CNF/GO aerogel, and selectivity of the MO/MB mixture using CNF/GO aerogel. Reprinted from (Nguyen et al. 2022). Open Access

for treating wastewater. In recent years cellulose/GO composites have received considerable interest as suitable adsorbents due to their unique properties high specific area, high porosity, and light weightness, as summarized in Table 5 (Wei et al. 2019).

The preparation of an aerogel composed of cellulose, GO, and nanochitosan result in a suitable material for oil removal from water bodies (Gu et al. 2021). In this case, the as-prepared aerogel through freeze drying was further heated at 150°C for an hour and cooled to ambient conditions to afford highly porous 3D aerogel. The aerogel exhibited low density, high hydrophobicity (i.e., water contact angle of 115.26°), and

oil adsorption capacities ranging between 120 g g⁻¹ to 171 g g⁻¹ depending on the oil type. The functionalized NPs can also be introduced into CNF/GO composites in order to improve the overall oil removal efficiency. Hui et al. (2021) demonstrated that the addition of amino-functionalized multi-walled carbon nanotubes (MW-CNTs-NH₂) can enhance the hydrophobicity property, and thus the adsorption capacity of the aerogel. The water contact angle increased from ~91° to 115° after the addition of MW-CNTs-NH₂. The aerogel exhibited excellent adsorption efficiency for different contaminants, such as ethyl acetate, dichloromethane, cyclohexane, acetone, and sesame oil, respectively.

Emerging pollutant and pesticide removal

The exponential world population growth demands high-quality and huge quantities of food. This has resulted in more of the agricultural sector relying heavily on herbicides and pesticides in order to maximize their production and quality of food. Although the use of these substances increased the production and quality of food produced, they have substantially affected the quality of our environment and pose a threat to animal and human health. Graphene-based aerogel materials have been deployed for the detection and extraction of various pesticides. To our knowledge, there is no research based on the utilization of CNF/GO hybrid for pesticide removal.

Despite numerous research works indicating that CNF/GO materials can be applied for the degradation of emerging pollutants including some pharmaceutical drugs, there are very few studies based on the adsorption of emerging pollutants (Anirudhan and Deepa 2017). Pharmaceutical companies play an essential role in our lives by manufacturing different drugs to improve our health and well-being. Most of the components of these drugs are excreted from our bodies into the environment. These chemicals can pass through the separation systems that are commonly used to remove different pollutants. The design of novel systems with suitable functionalities for targeting these chemicals is of the essence to protect the environment. The use of CNF/GO can benefit the removal of these components by introducing different functionalities specifically targeting them from contaminated systems. The availability of hydroxyl groups from CNFs and oxygenated groups from GO opens up the opportunity to introduce specific functionalities that can target these substances. CNF/GO/ZnO hybrid was employed for the removal of antibiotic drugs through the adsorption process (Anirudhan and Deepa 2017). It was reported that an increase in adsorbent dosage resulted in the increase in adsorption efficiency because of abundant available active sites. In the case of solution pH, it was noticed the adsorption efficiency increased with pH values up to 5.5, thereafter there was a gradual decrease. This results from strong electrostatic interaction between active sites from hybrid and lone pairs of electrons and fluorine found on the surface of ciprofloxacin.

Factors affecting pollutant removal efficacy of CNF/GO materials

The adsorption performance of CNF/GO hybrid composites can be viewed from various factors, including the proportion of components, their functionalities, preparation method or resulting form or shape. For example, aerogels offer porous materials leading to exposure of active binding sites for pollutants, while maintaining structural integrity (Abouzeid et al. 2022). In addition, the experimental conditions (e.g. pH, temperature, pollutant concentration, content of adsorbent, static or dynamic system) are also essential because the ionization of the functional groups relies on these conditions (Abouzeid et al. 2022). For instance, the hydroxyl and carboxyl groups are more ionizable at high pH values to form negative charges that are responsible for the adsorption of different pollutants, especially through electrostatic interaction (Abouzeid et al. 2022). GO exhibits high adsorption capacity depending on the modification applied. For instance, GO obtained from expandable graphite followed by oxidation using nitric acid exhibited MB adsorption capacity of 270.3 mg g⁻¹ (Li et al. 2013), whereas oxidation using hydrogen peroxide followed by freeze drying to afford GO aerogel resulted in maximum adsorption of MB reaching 416.7 mg g⁻¹. The oxidized GO showed a maximum MB adsorption ranging between 48–599 mg g⁻¹ depending on the extent of oxidation (Yan et al. 2014). The oxidation of GO increase in several non-aromatic carbon regions, and surface oxygen-containing functional groups which positively contribute to the adsorption efficiency. Graphite forms parallel π - π interaction with MB, while highly oxidized GO leads to MB to stand vertically on the GO plane through electrostatic interactions. The main concern is the stability of GO in water which may result in secondary pollution in water, hence reinforcing GO with eco-friendly materials is the facile solution to address this issue. Cellulose nanomaterials have been employed as suitable hosts to afford highly stable CNF/GO composites for adsorption purposes. These materials can be isolated from different sources using a wide variety of processes. These processes result in CNFs with different surface functional groups. For instance, the use of the H₂SO₄ hydrolysis process results in a large number of -OH and -SO₃ on the surface of the particles. The isolation process can be chosen depending on the

functional groups required for the intended application. The TEMPO oxidation process is the most commonly employed process for introducing carboxylate groups with some hydroxyl groups which are essential for adsorption application. The adsorption efficiency of the composite materials depends largely on the preparation method. Aerogels are a good example of a preparation method that produces materials with high porosity, mechanical strength, and low density. These properties enable access to the active sites and the stability of the composite in aqueous media.

Sensing applications

Sensor devices are composed of specialty electronics or otherwise sensitive materials that are capable of detecting a physical presence as metals, gases, or chemicals. These devices utilize materials with unique, intrinsic properties that allow the development of various types of sensors. Hence, sensors have been utilized in various applications such as healthcare, genetic analysis, environmental screening, and food safety testing. Based on the type of material used, these sensors can give an electrical and/or optical signal as an output. Electrochemical sensors or biosensors normally produce electrical signals with voltage, current, and conductivity as an output, while optical sensors are activated by light rays. A brief discussion of some selected sensors and the suitable types of materials are discussed below (Table 6).

Optical sensors

Optical sensors are used to evaluate any changes in the materials' optical properties (e.g. colour, absorbance, fluorescence, refractive, and reflectance index) in the presence of the analyte, hence can be employed for monitoring different analytes (Teodoro et al. 2021; Zhang et al. 2017). These sensors are mostly employed because of their attractive attributes, such as ease of operation, high precision, and rapid screening. In addition, they can be used in real-time, multiplexed, and for remote sensing applications. Nanocellulose-graphene-based materials have been employed in optical sensors using different techniques, i.e. surface-enhanced Raman scattering (SERS), as was recently discussed in great detail (Brakat and Zhu 2021; Ruiz-Palomero et al. 2017; Daniyal et al. 2020). This results from the exploitation

of chiral nematic features of nanocellulose materials, especially CNCs. Daniyal et al. (2020) prepared a thin film composite composed of gold modified with a CNC/GO layer using the spin coating method for metal ion sensing. The authors used surface plasmon resonance (SPR) as an optical sensor to evaluate the binding events for metal ion sensing, as shown in Fig. 8. The reference angle of 54.67° for deionized water was used to monitor any changes in the angle due to binding of metal ions (Cu and Zn) onto the substrate. It was found that the resonance angle was $54.77\text{--}55.14^\circ$ when concentration was increased from 0.01 to 1 ppm, and for Zn species the angle shifted from 54.84 to 55.03° (see Fig. 8b and c). This phenomenon was attributed to the electrostatic interaction between metal ions and substrate due to the presence of sulphate (SO_3^-) and carboxylic (COO^-), as shown in Fig. 8d. In another study, CNC was modified with hexadecyltrimethylammonium bromide for Cu^{2+} sensing using SPR (Daniyal et al. 2018a, b). It was reported the as-prepared sensor had a detection range between 0.01–0.5 ppm with a sensitivity of $3.271^\circ\text{ppm}^{-1}$ in aqueous solutions containing Cu^{2+} at concentrations ranging between 0.01 ppm to 60 ppm. Using the Langmuir model the binding affinity of Cu^{2+} towards the as-prepared thin film was found to be $4.075 \times 10^3 \text{ M}^{-1}$, compared to 0.99 M^{-1} for the neat gold film. This demonstrates the applicability of these thin films as a substrate for SPR sensing metal ions in water at fairly low concentrations when compared to neat gold with $\text{LOD} < 100$ ppm. The latter is because the refractive index value of water is almost equal to that of metal ions, and thus the modification of such substrate is of significance to enhance the sensitivity.

Electrochemical sensors

Electrochemical sensors are classified as chemical sensors in which an electrode is used as a transducer element in the presence of analytes. In this respect, an electrical sensor monitors any changes in electrical properties (e.g. an increase or decrease in electrical current or variation in voltage), while an electrochemical sensor converts the interaction of the analyte-electrode resulting from oxidation or reduction into an electrical signal. The sensitivity of electrochemical sensors depends on the type of electrode materials used. Thus, different types of materials ranging from metals, metal oxides, polymeric, and carbon-based materials have been explored as electrode materials.

Table 6 Summary for CNF/GO hybrid materials for sensing applications

Materials	Preparation method	Form	Target	Detection method	LOD	Linear range	Recovery (%)	Refs
CNF/graphene/polyamide	Immersion	CNF/GO coated nanofibrous mats	Hg ²⁺	Differential Pulse Voltammetry (DPV)	0.52 μM	2.5–200 μM	86–94	(Teodoro et al. 2019)
Nylon 6,6/Chitosan/CNF:rGO	Immersion	CNF/rGO coated nanofibrous mats	Isoborneol	Electrical impedance spectroscopy	25 ng L ⁻¹	-	-	(Migliorini et al. 2019)
CNF-pencil graphite	Immersion	Film	Atrazine	VC	0.008 ng L ⁻¹	5.0–320 ng mL ⁻¹	98–99	(Annu et al. 2020)
CNF-GO-nanoplatinum	Vacuum filtration followed by GO and then nanoplatinum	Film	Glucose	VC	0.08 ± 0.02 μM	0–500 μM	-	(Burrs et al. 2016)
		Film	E.coli	-	3.5 ± 1.1 CFU mL ⁻¹	10 ² –10 ⁷ CFU mL ⁻¹	-	
Hexadecyltrimethylammonium bromide modified CNF/GO	Spin coating	Film	Cu ²⁺	SPR	0.01 ppm	-	-	(Danialy et al. 2018b)
CNF/GO	Spin coating	Film	Cu ²⁺ and Zn ²⁺	SPR	0.01 ppm	-	-	(Danialy et al. 2020)

Amongst these, carbon materials such as graphite, carbon nanotubes, and graphene materials are the most employed due to their high surface area, electrochemical conductivity, and ability to host other materials, thereby forming composite materials with improved electrochemical properties. Graphene-based materials were used as decorators to promote the detection of cellulose-based materials. On the other hand, CNF/GO hybrid materials have also been successfully applied in electrical and electrochemical for the detection of various analytes (Zheng et al. 2019; Teodoro et al. 2019). The use of nanocellulose and GO in both electrical and electrochemical sensors is due to their attractive attributes, such as high thermal stability, large surface area, high aspect ratio, excellent mechanical properties, and optical properties.

For instance, in their study by (Zheng et al. 2019), investigated the role of nanocellulose and graphene in the poly(vinyl alcohol)-borax (CNF/GN@PVA) hydrogel for sensing devices. It was reported that borax acted as an interlinker between PVA and CNF/GN enhancing the flexibility and toughness of the hydrogel, meanwhile, CNFs facilitated the dispersion of the GN such that the mechanical performance and conductivity were remarkably improved. The resulting hybrid composite with high toughness, rapid self-healing ability, and efficiency was suitable for wearable sensing devices. The presence of CNF-GN provided excellent electric pathways which afforded their integration with strain sensors with remarkable responsiveness, stability, and repeatability which enable identification of various human motions with the

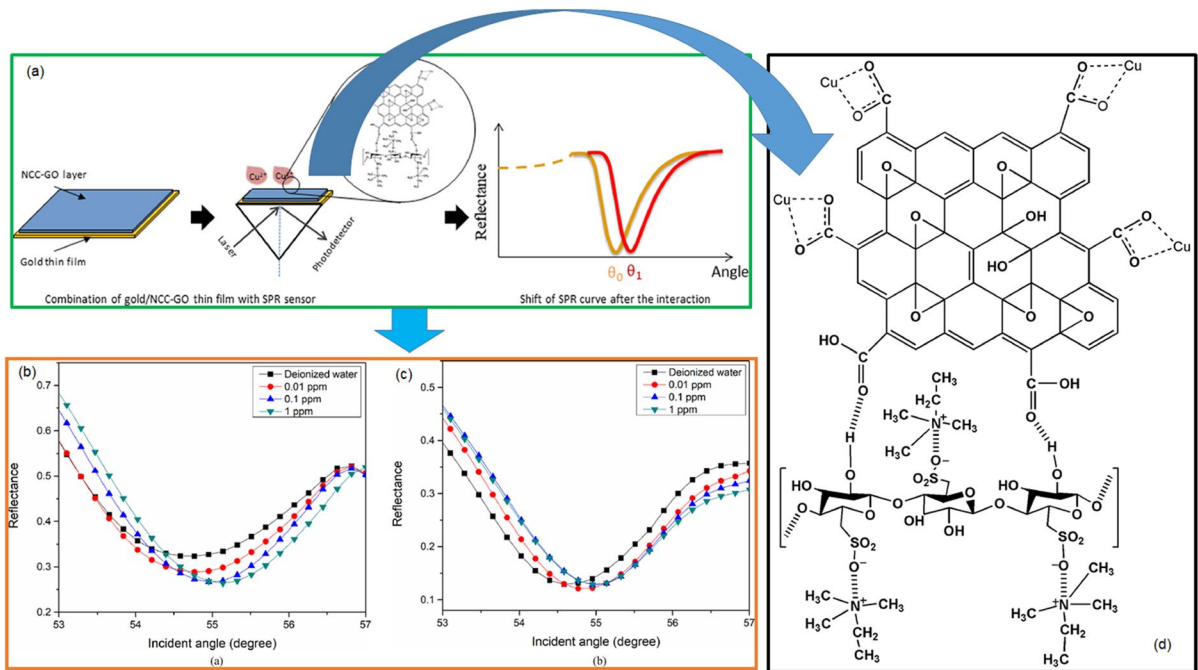


Fig. 8 a Schematic illustration of SPR result during the interaction with metal ions. SPR response for thin film in contact with (b) Cu^{2+} and (c) Zn^{2+} . Possible electrostatic interaction

between metal ions and the as-prepared thin film substrate. Reprinted with permission from (Daniyal et al. 2020)

gauge factor GF of ~ 3.8 which can be applied in sensing wearable devices.

Teodoro et al. (2019) reported on the preparation of an electrochemical sensor for Hg^{2+} composed of CNC, rGO, and polyamide (PA) via immersion process. CNC surface functionalities were exploited as reducing agents for GO's oxygen organic functions to afford highly dispersed GO on the surface of CNC. It was reported that 2 h of immersion of electrospun PA into CNC:rGO was sufficient to afford a high electron transfer rate and low peak potential separation (ΔE_p). The sensor was able to detect Hg^{2+} with a low limit of detection (LOD) of $0.52 \mu\text{M}$ with high selectivity in the presence of other pollutants (i.e. Cd^{2+} , Pb^{2+} , and Cu^{2+}). Using real water samples, viz. tap and river water samples, the device was capable of detecting Hg^{2+} ($50 \mu\text{M}$) with recovery tests from 97% for river water and 102% for tap water. A dynamic linear range of 2.5–200 μM Hg^{2+} sensing using DPV in real water samples indicates this type of device can be used for environmental sensing applications. In the work by Migliorini et al. (2019) developed an electronic tongue (e-tongue) sensor array composed of

CNC, rGO, nylon, and chitosan for the detection of isoborneol. In this regard nylon/chitosan was electrospun onto a gold interdigitated electrodes (IDE) substrate followed by immersion into CNC:rGO. The hybrid material possessed high electron transfer efficiency due to high electrical conductivity and differentiated and detected isoborneol down to an LOD of 25 ng L^{-1} . In addition, the sensor was capable of detecting isoborneol in river water indicating this hybrid materials have a vast potential in sensing applications. Pencil graphite was also reported as a source of graphite to decorate nanocellulose for the detection of the analytes. Elsewhere, a sensor for the detection of herbicide atrazine (ATZ) was fabricated by using pencil graphite and nanocellulose composite material (Annu et al. 2020). A low detection limit of 0.008 ng mL^{-1} was attained.

The inclusion of biological molecule as element responsible for recognition in a sensors has been also reported (Teodoro et al. 2021; Zhang et al. 2017). These biosensors are usually composed of nanomaterials to increase stability with excellent selectivity. These nanomaterials serve as substrate for

immobilizing and stabilizing the biomolecules, viz. enzymes, antibodies, proteins, peptides aptamers, nucleic acids etc. for detection purposes (Teodoro et al. 2021). Since there are number of issues raised on the use of nanomaterials with regard to their cytotoxicity, cellulose-based nanomaterials serve as green alternative NMs for stabilization and immobilization for biomolecules. Point of care biosensing device for glucose or *E. coli* was developed by combining CNF, GO, and nano-platinum (Burrs et al. 2016). In this work, GO-coated CNF was reduced through thermal and chemical treatment and decorated with cauliflower-like nanoplatinum obtained from the pulsed sono-electro-deposition process. The functionalization of the obtained hybrid composite with glucose oxidase (i.e., via chitosan hydrogel encapsulation) or with RNA aptamer (i.e., via covalent bonding) to afford a point of care biosensor for glucose and *E. coli* sensing purpose. The device had a detection limit of $0.08 \pm 0.02 \mu\text{M}$ and 0157:H7 ($\sim 4 \text{ CFU mL}^{-1}$) with a response time of 6 s and 12 min for glucose and *E. coli*, respectively. It was found that the as-prepared CNF/GO-nanoplatinum-based sensor with comparable response time and detection efficiency to the commercially available biosensors is reliable for electrochemical sensing devices for preferably small molecules.

Wearable sensors

Technological advancements have seen most researchers paving the way for devising wearable devices that are essential for our well-being (Horta-Velázquez and Morales-Narváez 2022; Li et al. 2022; Lu et al. 2021; Cong et al. 2013). For instance, these devices are often used in healthcare systems to monitor, process, and transmit data that can be utilized in order to make informed decisions. They are also used for other purposes such as monitoring environmental safety (toxic gases exposure), UV exposure, biosignals (sweat), etc. Nanocellulose has been utilized as one of the critical components of wearable sensors because of its unique features such as ease of processability, good mechanical properties, lightweightness, sustainability, and ease of modification to afford desired electrical and optical properties essential for attaining anticipated stimuli response (Horta-Velázquez and Morales-Narváez 2022). The properties of the sensing device are directly dependent

on the targeted activity in which the device will be employed. For instance, stretchable devices with rapid response are essential for detecting movements from lower and upper limbs.

The wearable devices have to withstand mechanical deformation with acceptable sensitivity to monitor or detect any targeted movements. Although nanocellulose has been applied for developing wearable devices, its limited electrical conductivity has been the major challenge. The inclusion of GO improves conductivity and mechanical properties to afford reliable sensing devices in real-time human motion detection (Liu et al. 2021). Liu et al. (2021) developed a self-healing and self-adhesive strain-sensing device composed of PVA/rGO/tannic acid (TA)-decorated CNC/ polydopamine (PA). Tannic acid decorated CNCs as dynamic motifs were incorporated into PVA polymer in the presence of PDA-reduced rGO for conductive as well as borax for crosslinking purposes (Fig. 9). The resulting hydrogel displayed high stretch-ability and good self-healing even after being torn into two pieces. This behaviour was ascribed to the presence of reversible dynamic catechol-borate bonds from CNC/TA and supramolecular interaction between CNC/TA, PVA, rGO, and PA (Fig. 9a). The catechol groups of TA on the surface of the as-prepared hydrogel afforded distinctive self-adhesive to various surfaces, as shown in Fig. 9a. The presence of rGO enhance the electrical conductivity of the composite material. As anticipated the electrical conductivity increased with rGO content up to 4% rGO, after which a decline in conductivity was recorded. The detection of human movement by attaching the sensor onto the finger, wrist, elbow, and knee, it was demonstrated that the as-prepared sensor exhibited reliable data associated with the movements of the targeted part bending and stretching (see Fig. 9b). The sensor was capable of detecting all motions even speaking (Fig. 9c), with remarkable reusability due to self-healing process with no discernible deterioration. In their work, Li et al. (2022) devised a novel hydrogel for strain-sensing application. In this case, the authors incorporated poly(N-vinylpyrrolidone)-grafted-CNC (PVP-g-CNC) and rGO-grafted with poly(acrylic acid) rGO-g-PAA into polyacrylamide (PAM) hydrogel network via in situ free radical polymerization to afford highly resilient, conductive, and tough material. It is noteworthy to mention that the inclusion of CNCs and rGO is essential for

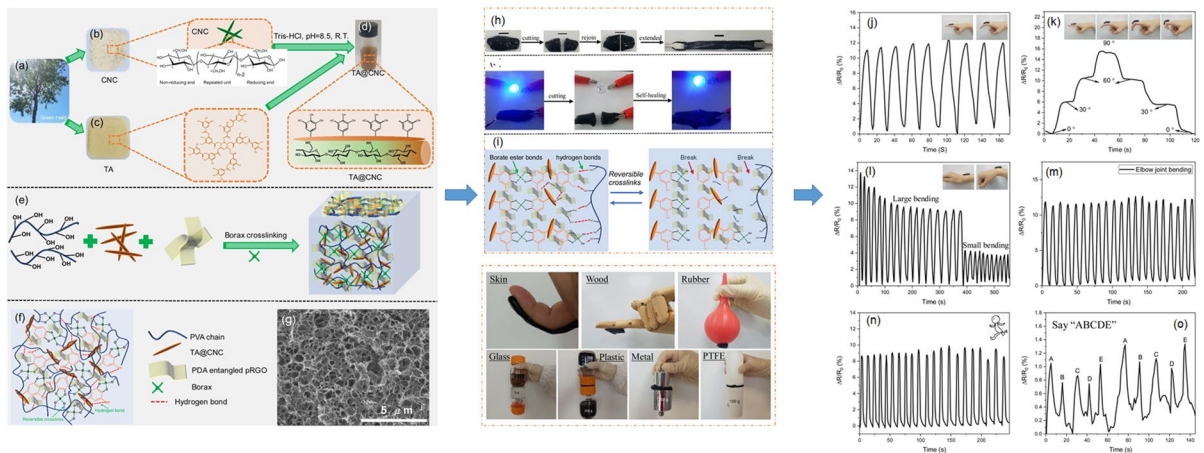


Fig. 9 a–g Schematic illustration for preparation of hydrogel strain sensing device. h stretch-ability, self-healing and self-adhesive of the prepared hydrogel. Real-time human motion monitoring resistance changes in (Ghaee et al. 2019) finger movements, (l) wrist bending, (m) elbow joint bending, (n)

knee joint bending, and (o) voice detection. Reproduced with permission from (Xiaoyan Liu et al. 2021). The inserted glucose unit in (b) is reproduced with permission from (French 2017)

flexibility and mechanical response under stress. The as-prepared hydrogel exhibited elongation-at-break of 1224% and maximum tensile strength 297 kPa with resilience of higher than 95% after 10 cyclic tensile loading–unloading. Due to the good dispersion of rGO within the system that afforded the formation of the conductive pathway, the electrical conductivity increased with rGO content. The conductive and mechanical performance of the hydrogel translated into excellent strain sensitivity with a gauge factor ranging between 0.7–1.1 depending on the rGO content. The sensor exhibited good human motion detection when attached to a finger or wrist. This demonstrated that the as-prepared composite can be employed for flexible strain sensing because of high conductivity, high resilience, and good toughness, which led to good cycling stability and repeatability.

In terms of pressure sensor sensitivity is a more important factor than the stretch-ability of the hybrid composite material (Wang et al. 2019). Despite the combination of GO and CNFs being used to fabricate carbon aerogels for pressure-sensing applications, there were no studies that are directly based on nanocellulose and GO composites (Wang et al. 2019). It is worth mentioning that the carbon aerogel prepared from these materials exhibited high conductivity reaching values of 181 S m^{-1} , strong

fatigue resistance, acceptable compressive stress, and a detection process (Wang et al. 2019). The success of these materials lies in the fact that during compression or under pressure the electrical resistance decreases due to carbon molecules coming closer and proving conduction pathways within the system (Wang et al. 2019). Elsewhere, it was reported that the as-prepared carbon aerogel displayed high compressibility of $\sim 90\%$ and high fatigue resistance at 50% strain within 10 000 cyclic compressive loading–unloading. The resulting aerogel had a density of 3.26 mg cm^{-3} and electrical conductivity of 0.32 S m^{-1} that afforded a sensitivity of 0.26 kPa^{-1} .

Humidity sensors

The synergy between nanocellulose and GO was also explored for novel renewable, flexible, and cheaper humidity sensors (Kafy et al. 2016; Xu et al. 2016a). Humidity sensors are essential for monitoring and controlling humidity in various sectors such as agriculture for greenhouse air control, and soil monitoring, healthcare for medicine processing, automotive for window defoggers, households for smart cooking controls in microwave ovens, and smart laundry control, etc. A mixture of GO and nanocellulose at a preferable ratio was homogenized followed by oven drying

to develop a film for a highly selective humidity sensor (Kafy et al. 2016). The sensing device was devised by depositing an interdigital transducer (IDT) patterned electrode onto a PET substrate. Subsequently, the composite suspension was poured on the patterned electrode and then dried in an oven to afford its wiring to connect it to an LCR meter for sensing measurement, as shown in Fig. 10. The as-prepared film exhibited linear and excellent response. In addition, the increase in temperature did not influence the responsiveness or performance of the sensor indicating that it can be used for humidity detection in flexible and wearable electronics (see Fig. 10). In this case, the sensing behaviour of the composites can be associated with the presence of a large number of hydroxyl groups from both GO and CNC making the composite more hydrophilic. In addition, GO contributes to carboxyl groups to increase the hydrophilicity property that is responsible for the attraction of water molecules, and thus improves the humidity sensitivity of the composites.

Xu et al. (2016a) developed a humidity sensor from a hybrid of PVA/rGO/CNFs. In this case, CNFs promoted the dispersion of rGO in water due to electrostatic repulsion between the fibrils, meanwhile mixing the suspension with PVA afforded freestanding films through solvent evaporation.

The conductivity of the hybrid was enhanced and promoted the sensitivity and changes in relative humidity (RH) with excellent repeatability with RH ranging between 50–70%. CNFs can serve as compatibilizers to improve rGO interfacial adhesion and dispersion in PVA, as a bridge to promote load transfer and humidity transfer between hybrid components, and as water absorbers to improve the overall humidity sensitivity.

Other sensors

Besides the fact that cellulose decorated with other nanomaterials (NMs) (e.g. zinc oxide, titanium oxide, iron oxide) have been explored for gas sensing purposes, very few studies have been dedicated to investigating the combination of cellulose and graphene for such purposes (Basu and Bhattacharyya 2012; Dacrory et al. 2022). A recent study by Dacrory and colleagues demonstrated that cellulose and GO composite can be used for ammonia gas in the presence of EDA as a crosslinker (Dacrory et al. 2022). The composite exhibited excellent sensing properties for ammonia from 5–100 ppm at room temperature. It was noticed that the use of 1.5 mmol EDA as a crosslinking agent resulted in superior response because when the EDA content is used

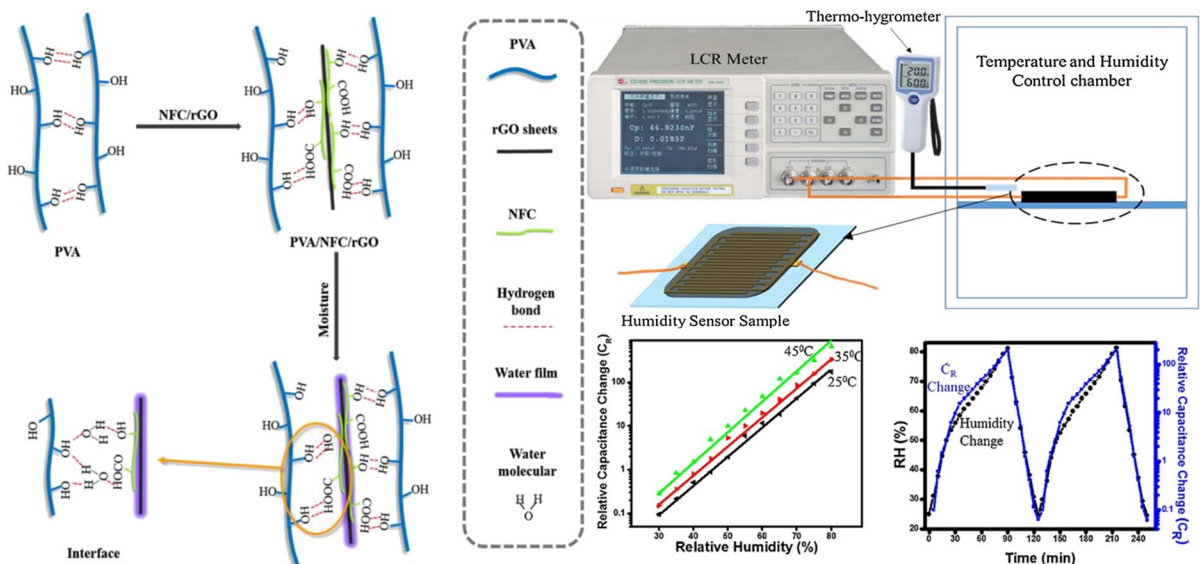


Fig. 10 Schematic presentation for the role played by CNFs within the hybrid composites-based sensors (left-hand side) (Xu et al. 2016a). Schematic illustration of humidity sensing device to measure its performance. Relative capacitance vs

humidity at different temperatures, and (c) relative humidity with time (right-hand side). Reprinted with permission (Kafy et al. 2016)

the available $-\text{COOH}$ from GO responsible for higher response is consumed through reaction with EDA. The response and recovery times were 490 s and 620 s, respectively.

Factors affecting the sensing properties of CNF/GO hybrids

The presence of GO enhances the conductivity of the composite materials, but their an optimal content to afford the percolation threshold to form an insulator-to-conductor transition. On the other hand, nanocellulose offers a platform to enhance the dispersion of GO due to the strong interaction between GO and CNF. The electrostatic repulsion between fibrils is responsible for improving the overall dispersion of GO by acting against van der Waals forces between GO nanosheets. For instance, nanocellulose with a large number of hydroxyl groups afford the attachment of water molecules via hydrogen bonding, and these bonds act as channels for facilitating water molecules to form or deform water molecular film that promotes the sensitivity and reduced hysteresis phenomenon (Xu et al. 2016a). In the case of sensor devices materials used to build such a system are of the essence to have high performance about selectivity, and specificity. Sensor devices are regarded as alternative analytical systems due to their compactness, and portability than the conventional methods. They can be applied for on-site monitoring and can be easily configured into different substrates. Hence, these sensors can be designed for medical, environmental, food safety, air monitoring, and wireless communication technologies. Optical, electrochemical, pressure, and humidity sensors are all dependent on the type of materials used as a sensing platform. The use of nanocellulose (CNFs)-based materials offers considerable properties due to their environmental friendliness, flexibility, and disposability. These features allow the use of CNF materials in emerging wearable technology. In cases where flexibility is not the concern, the sensitivity of CNF-based sensors has been improved by the incorporation of GO materials due to their high electrochemical conductivity and fast electron transfer kinetics. It has been noted that the change in morphology and flexibility of CNF/GO-based materials also resulted in better sensing signals.

This allows further investigation of various methods for the synthesis of CNF-based materials as suitable materials with better flexibility.

Energy storage/conversion

Supercapacitors

Energy harvesting and storage have been topical subjects over the past decades. The utilization of cheaper and accessible materials for such purposes received attention from both industrial and research communities (Ikram et al. 2020; Xiong et al. 2021). The realization for production of GO production from laboratory scale to industrial scale as well as the use of recycled materials makes GO one of the interesting materials for energy storage applications (Ikram et al. 2020). However, GO suffers from processability, and high production cost. Therefore, GO are used as additive to qualify for energy storage applications. The combination of cellulose nanofibrils with GO can improve processability while enhancing the energy storage efficiency (Ikram et al. 2020; Xiong et al. 2021).

The simplicity of functionalization of the CNF/GO hybrid composites and different structural forms offers the opportunity to develop advanced supercapacitors for energy storage applications. CNFs play an essential role in enhancing the performance of the supercapacitor (Liang et al. 2022). This results from the formation of a 3D porous structure from intra- and intermolecular hydrogen bonds that accommodate more ion absorptive sites and more diffusion channels for ease of charge transfer (Liang et al. 2022). In addition, the presence of GO in the hybrid system increases the conductivity meanwhile the CNF serves as a spacer that prevents aggregation of GO and provides the resultant material with excellent mechanical performance including mechanical strength and flexibility (Xiong et al. 2021). CNF/GO hydrogel was developed using the one-pot hydrothermal method for energy storage applications (Zhang et al. 2022). The highly porous hydrogel with a specific surface area offered ultrahigh gravimetric capacitance of 342.5 Fg^{-1} and volumetric capacitance of 339.1 Fcm^{-3} at 0.3 Ag^{-1} due to high packing density, high porosity, and the availability of heteroatom functional groups. (Mo et al. 2018) used CNFs to provide strength and prevent the restacking of graphene sheets

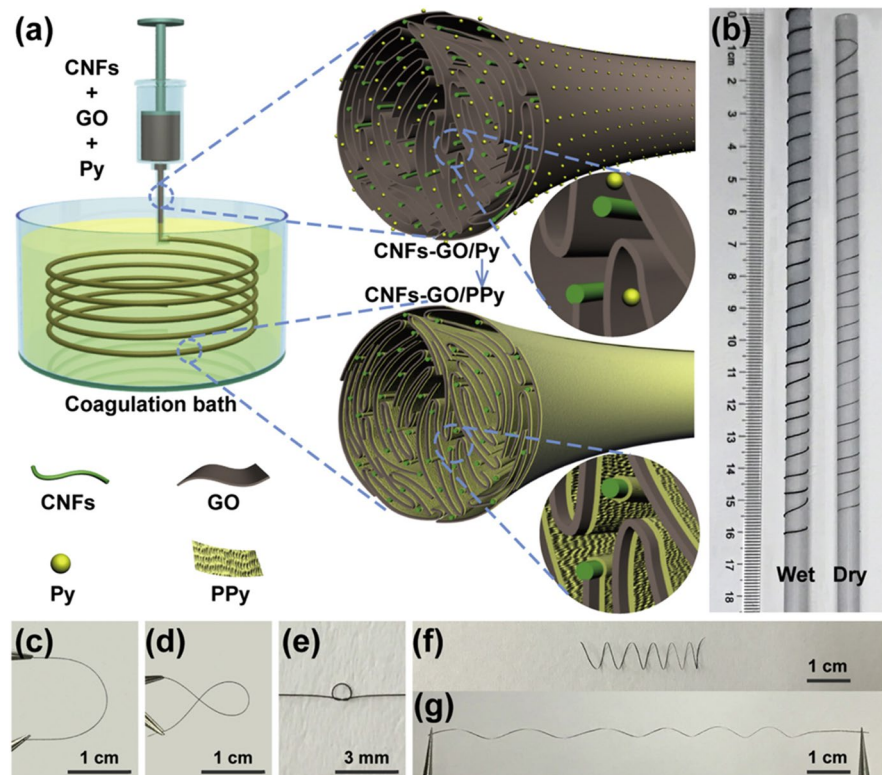
for fibre-shaped supercapacitors. Wet-spinning was employed to fabricate microfibers that are flexible capable of bending, being a knot, and stretched without any damage (Fig. 11). The CNFs were isolated from bamboo fibres through chemical and mechanical methods. The as-prepared hybrid fibres exhibited superior mechanical strength (364.3 MPa) and an acceptable elongation-at-break of 2.9%. The hybrid areal-specific capacitance reached 334 mF cm^{-2} at the current density of 0.1 mA cm^{-2} in a liquid electrolyte, which corresponds to the length and volumetric capacitance of 4.2 mF cm^{-1} and 334 mF cm^{-2} . It reached an energy density of $7.4 \text{ } \mu\text{Wh cm}^{-2}$ and a volumetric density of $20 \text{ } \mu\text{Wh cm}^{-3}$ while maintaining 100% of the initial capacitance after 2000 charge-discharging cycles. On the other hand, the specific capacitance reached 218 mF cm^{-2} which corresponds to a length capacitance of 2.7 mF cm^{-1} volumetric capacitance of 218 mF cm^{-2} , energy density of $4.8 \text{ } \mu\text{Wh cm}^{-2}$ and volumetric density of 4.8 mWh cm^{-3} . The as-prepared hybrid retained 95% of initial capacitance after 3000 charge and discharge cycles indicating stability, even after bending for 3000 cycles it maintained the same capacitance.

Xiong et al.(2021) reported that CNFs provided the resultant hybrid films with flexibility with tensile strength increasing by 787% when compared to pure GO-based film. The authors demonstrated that the resultant film can be assembled into a symmetrical supercapacitor with good stability, and excellent rate performance. The as-prepared CNF/GO film exhibited a specific capacitance of 120 mF cm^{-2} (242 Fg^{-1}), energy efficiency of 80%, energy density of $536 \text{ } \mu\text{Wh cm}^{-2}$ (32 Wh kg^{-1}), and power density of 193 mW cm^{-2} (53 kW kg^{-1}). The improved properties were attributed to CNF serving as an excellent spacer to promote GO dispersion and thus large specific surface area to store more charges. In addition, cross-linked CNFs form porous structures providing sufficient space and channels for storing and facilitating of charges transportation.

Phase change materials

Phase change materials (PCMs) are recognized by their capability to store and release thermal energy during the phase change process (Mochane and Luyt 2012; Yang et al. 2016; Zhu et al. 2023). These

Fig. 11 a Schematic representation of the fabrication process for CNF/GO/polypyrrole (PPy) microfibers. b Images for microfibers under wet and dry conditions. (c-g) Microfibres under different mechanical strains (Mo et al. 2018)



materials are commonly employed in energy fields as latent heat energy storage and release medium for thermal management applications. Organic PCMs, such as polyethylene glycol, paraffin wax, and alkenes are the most widely used PCMs. The leakage of organic PCMs during solid-to-liquid phase transition and poor thermal conductivity are some of the limitations that hinder their wide application. Over the past decades, different supporting materials such as polyethylene, polypropylene, and graphite have been employed to overcome the leakage during the phase transition process. In addition, a variety of thermally conductive fillers have been incorporated into the system to improve the resultant heat transfer efficiency. GO and CNFs can serve as a supporting material for the encapsulation of the PCMs. In addition, the presence of GO enhances the thermal conductivity, thus facilitating heat transfer within the system (Qiu et al. 2024). Qiu et al. (2024) prepared a multifunctional composite material utilizing an oil-in-water Pickering emulsion, by combining CNF/GO with paraffin wax. To prepare aerogel film, the resulting mixture was freeze-dried. This demonstrates that phase change materials can be encapsulated using CNF/GO for heat management applications. In the presence of CNF and GO, cellulose-6(N-pyridinium)hexanoyl ester was used to create a porous PCM composite capsule that contained polyethylene glycol (Li et al. 2023). PEG was satisfactorily contained in the resulting composite material up to 34 g g^{-1} . The latent heat up to 142 J g^{-1} , or 98% of clean PEG, was reached and the thermal conductivity was significantly improved. With latent heat values and DSC curves remaining unchanged after 200 heating and cooling cycles, the as-prepared PCM composites demonstrated good stability. Despite these intriguing qualities, the majority of research focuses on carbonizing CNF/GO/PCM to create PCM composites that are thermally conductive for a range of uses, including solar-thermal energy conversion (Qiu et al. 2024; Min et al. 2018; Zhu et al. 2023; Hekimoğlu et al. 2023). Thus, it is imperative that researchers investigate the application of these composites.

Composites

CNF/GO hybrid can be used as nanofillers in polymers to produce multifunctional composites for various applications (Jia et al. 2020; Javadi et al. 2013).

The presence of these nanofillers improves thermal, mechanical, and UV-shielding properties (Jia et al. 2020; Javadi et al. 2013). In addition, the reduction in moisture absorption has been reported in some of the studies based on moisture-sensitive polymers (Jia et al. 2020; Akindoyo et al. 2019; Javadi et al. 2013). Jia et al. (2020) reported that the addition of 5% CNF/GO as filler for PVA reduced moisture absorption by ~50%, whereas the mechanical strength increased by ~75% and modulus increased by 278%. The UV-shielding performance was enhanced from 65 to 99%. CNC/GO was also employed as a reinforcing agent for PVA to afford thermal stable and transparent materials (Montes et al. 2015). The presence of the fillers resulted in enhanced mechanical performance, excellent thermal stability, and high transparency. This indicates that multifunctional composites can be manufactured to afford their application in various fields depending on the host polymeric materials. Depending on the processing methods different forms of hybrid composites can be attained that can afford their application in various fields (Javadi et al. 2013). Hybrid aerogel composed of PVA, CNFs, and GO was successfully prepared using freeze drying process by Javadi et al. (2013). The aerogel was treated with silane compounds, viz. silane 1, (tridecafluoro-1,1,2,2-tetrahydrooctyl trichlorosilane, and silane 2, (4trifluoromethyl-tetrafluorophenyl)triethoxysilane, to render the surface hydrophobic property. The as-prepared hybrid aerogel exhibited a series of remarkable properties, such as high porosity, ultra-low density, hydrophobic, high specific compressive strain and compressive failure strain, good thermal stability, and thermal conductivity which qualifies these materials for thermal insulation in homes, aerospace, smart textiles and automotive industries.

Other applications

CNF/GO hybrid composites have been employed in other applications due to their attractive attributes (Li et al. 2019; Shao et al. 2018). The presence of CNFs stabilizes GO, hence improves its dispersion with the system (Li et al. 2019; Shao et al. 2018). In addition, the resulting 3D structure and hydrophilicity of both CNFs and GO plays a critical role depending on the intended applications (Li et al. 2019; Shao et al. 2018). Yuan and co-workers from Guangxi University in Nanning reported on the use of CNF/GO hybrid

composite for electric heating membranes (Li et al. 2019). CNFs were obtained from wood-bleached sulphate pulp by treating with cellulose followed by high-pressure homogenization. A hybrid composite was prepared by mixing CNFs with GO suspension followed by sonication to afford better dispersion. The as-prepared composite was prepared via vacuum filtration followed by vacuum drying at 60°C for 12 h (see Fig. 12). The authors noticed that sheet resistance decreased exponentially with an increase in GO content within the hybrid composites. This was attributed to the good dispersion of GO within the samples. It was deduced that the GO sheets in the composite overlapped and were stacked in plane and parallel, thus providing contact points for steady heat conduction for electric heating. The hybrid was able to reach an equilibrium temperature of 60 within 3 min under 2000 W m^{-2} , which was found to increase linearly with the content of GO within the composite.

Graphene was introduced into the CNF/GO hybrid to enhance the overall performance of the composites (Shao et al. 2018). The increase in graphene content decreased sheet resistivity exponentially, while the increase in grammage linearly decreased sheet resistance of the heating membrane. The as-prepared hybrid composite exhibited no significant changes in the rate of resistance between the electrodes after 100–600 times bending. The balanced temperature rise was observed as the content of graphene was increased within the hybrid composite (Fig. 13a). This could be accounted for by the

conductive network generated by graphene sheets, which further overlap each other and increase in number of joints as the content increases. Therefore, this resulted in an increase in main electric heating with no significant changes in the change rate of resistance (CRR) at the second outage (Fig. 13b). In the case of grammage, it was noticed that changes in grammage had no significant variations with the rise in temperatures (Fig. 13c). It was also deduced that temperature rise in a plane electric heater displayed exponential trend (Fig. 13d).

Elsewhere, the inclusion of GO into CNFs resulted in composites with excellent barrier properties (Ren et al. 2019). The authors used a combination of preparation methods, i.e. layer-by-layer coating and hot-pressing, in order to attain a highly oriented CNF/GO composite, as shown in Fig. 14. The tensile strength and modulus increased by ~ 2.1 (i.e., from 29 to 62 MPa) and 57.5 (i.e., from 0.08 to 4.6 GPa) times when compared to neat CNFs-based films. The permeability of O_2 (P_{O_2}) decreased with an increase in GO content due to strong interfacial adhesion between GO and CNFs as well as high orientation and compacted structure of GO sheets under high shear flow during layer-by-layer film coating. With the addition of 5% GO the P_{O_2} reduced to $1.4 \times 10^{-17} \text{ cm}^3 \text{ cm} \cdot \text{cm}^{-2} \text{ s}^{-1} \text{ Pa}^{-1}$, viz. approximately 4×10^4 times when compared to neat CNFs-based films. The presence of oriented GO along the hybrid composite film formed a tortuous path which prolonged the gas diffusion. Water vapour barrier property reduced by $\sim 32\%$ from

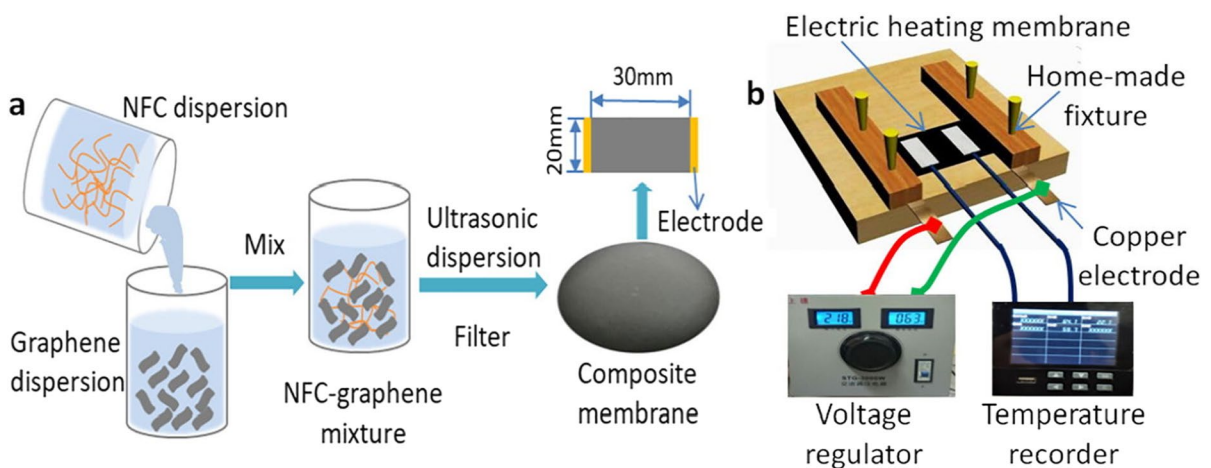


Fig. 12 Schematic representation for (a) preparation and (b) electric heating testing of CNF/GO hybrid composite (Li et al. 2019)

1.6×10^{-12} to 1.1×10^{-12} g cm cm⁻² s⁻¹ Pa⁻¹. The limited reduction can be associated with the hydrophilic character of both CNFs and GO.

A recent study by Yu et al. (2023) demonstrated that the inclusion of cellulose nanofibers into GO improved life extension and corrosion protection through the spraying process. The presence of CNFs improved mechanical performance and tribological properties of GO. This enabled the preparation of composite material that can coat steel resulting from synergy between GO and CNFs for affording tough and strong coating material due to strong interaction between CNFs and GO via hydrogen bonding from their COOH groups.

Challenges and perspectives

Despite research activities dedicated to the isolation of nanocellulose materials, the cost associated with nanocellulose is still a major issue. In addition, the most successful methods that afford the production of nanocellulose at an industrial scale use high energy and employ toxic chemicals (e.g., sulphuric acid) that have a negative impact on the environment (Mokhena and John 2020a; Teo and Wahab 2020). The utilization of green methods for the isolation of nanocellulose is still in the infancy stage and is of the essence to broaden their industrial application specifically from economic and ecological viewpoints. Such

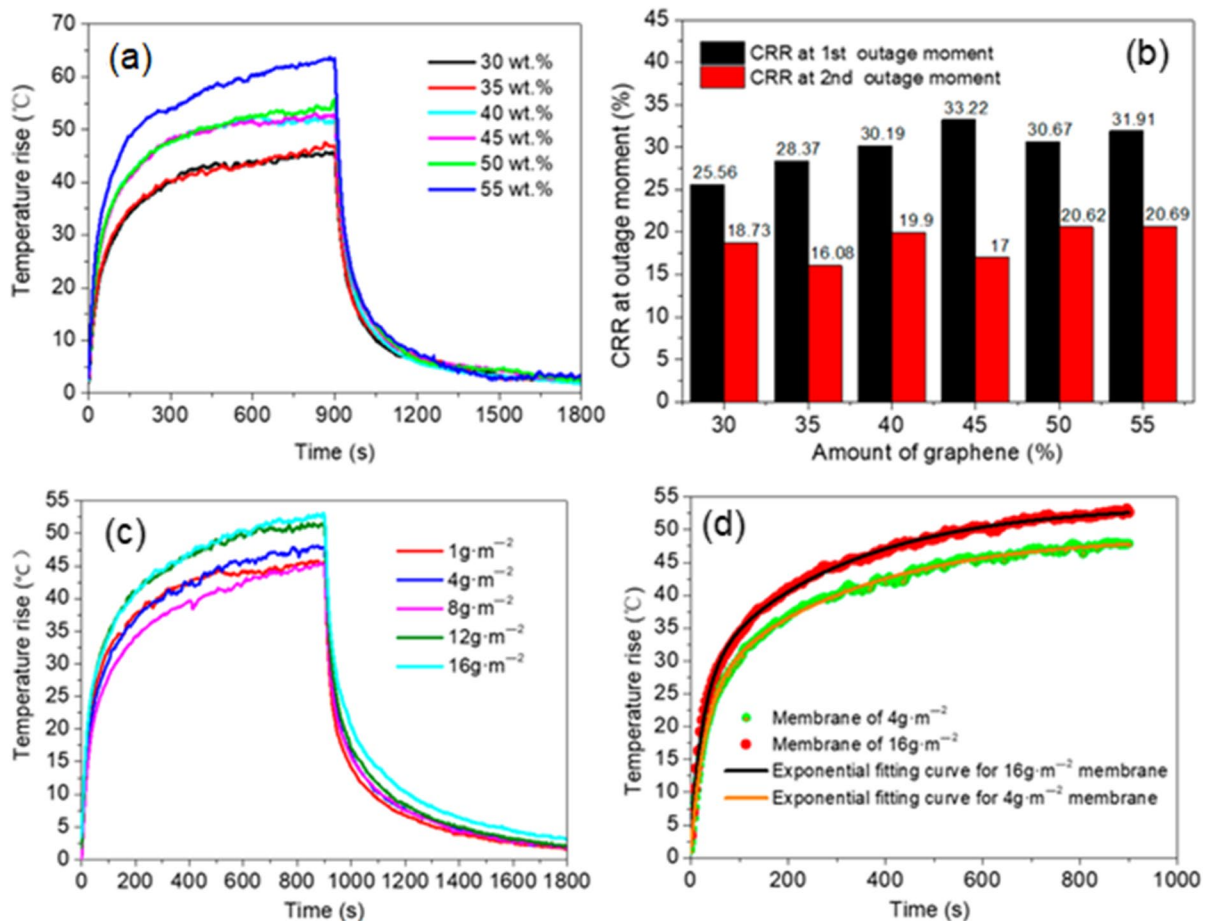


Fig. 13 Second heating test of the 16 g m⁻² hybrid composite containing different amounts of graphene. **a** Temperature rise and **(b)** change rate of resistance (CRR) at the outage moment.

c temperature rise hybrid composite/graphene membranes at different grammages, and **(b)** exponential fitting of the 4 and 16 g m⁻² composites (Shao et al. 2018). Open Access

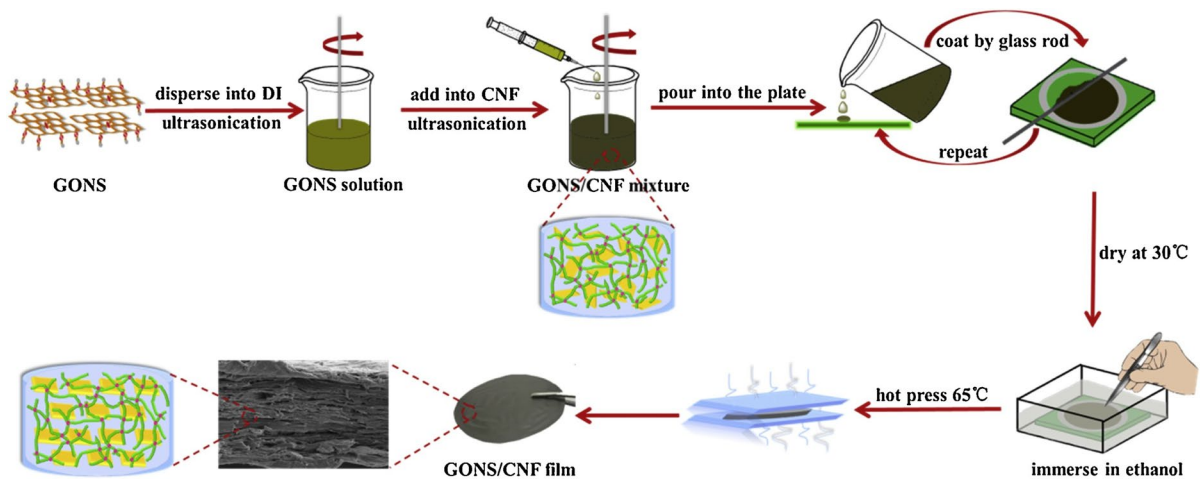


Fig. 14 Schematic illustration of the preparation method of CNF/GO hybrid composite (Ren et al. 2019)

processes will stamp the globally accepted perception of nanocellulose as green nanomaterials with comparable properties with other available materials (e.g. CNTs). Like other carbon-based materials, GO is prone to aggregation resulting from the van der Waals forces. This makes it difficult to achieve desirable GO dispersion within the system under investigation.

The integration of nanocellulose and GO serves as a suitable technique to improve the dispersion of GO and thus the overall properties of the resulting hybrid material. Moreover, nanocellulose is biodegradable and sustainable with exceptional mechanical properties, and a large specific area with a large number of hydroxyl groups and other functionalities, i.e. depending on the isolation process, that is responsible for strong adhesion and good dispersion of GO within the composite. It is worth mentioning that the selection of the method is essential to afford the production of the materials with anticipated architectural structure. This is of paramount importance from the application point of view. For instance, aerogel are highly porous which can be essential for oil removal purposes. One of the critical issues that still needs to be addressed is understanding the interaction between CNFs and GO in order to further enhance the properties of the resultant composite materials. The development of new methods that can afford the functionalization and fabrication of CNF/GO composites can significantly revolutionize their applicability beyond their traditional applications. It will lead to

the exploration of other applications such as optics, thermal management, electromagnetic shielding, and many more.

GO has limitations in serving as a good electrical and thermal conductor. The additional fillers that are more stable under harsh conditions such as MOFs/MXenes can improve the overall performance of CNF/GO hybrids, especially in electrochemical applications (sensors and energy devices). This is attributed to the fact that these materials have metal centres that can undergo oxidation–reduction reactions thereby ensuring fast electron transportation with minimal energy/voltage losses. In addition, MXenes and MOFs exhibit additional functionalities that can improve the adsorption of targeted pollutants due to their excellent surface area.

For the use of CNF/GO hybrids in the adsorption of new contaminants, more studies are still required. This research should focus on the production of various structural materials from these materials. The unique properties of nanocellulose, such as its superior mechanical performance and strong hydrogen bonds that prevent it from melting, have also been investigated for use in the encapsulation of phase-change materials; however, the addition of GO can further enhance the overall performance of such materials. The latter can be attributed to a significant interaction between GO and CNFs, which allows for GO dispersion and enhances the composite's thermal conductivity.

Acknowledgments Authors acknowledge Department of Science and Innovation (DSI)/Mintek Nanotechnology Innovation Centre, and Mintek for providing resources.

Author contributions T.C.-Project conceptualization and draft.

M.J.-Project conceptualization and draft.
A.-Writing and Proof reading.
S.-Writing and Proof reading.
B.-Writing and Proof reading.
E.G.-Writing and Proof reading.
L.-Writing and Proof reading.
T.S. -Writing and Proof reading.

Funding Open access funding provided by Mintek. The authors were funded in part by the Department of Science and Innovation (DSI)/Mintek Nanotechnology Innovation Centre, and the Mintek Science Vote Grant.

Data availability No datasets were generated or analysed during the current study.

Declarations

Ethical approval Compliance with ethical standards.

Competing interests The authors declare no competing interests.

Open Access This article is licensed under a Creative Commons Attribution 4.0 International License, which permits use, sharing, adaptation, distribution and reproduction in any medium or format, as long as you give appropriate credit to the original author(s) and the source, provide a link to the Creative Commons licence, and indicate if changes were made. The images or other third party material in this article are included in the article's Creative Commons licence, unless indicated otherwise in a credit line to the material. If material is not included in the article's Creative Commons licence and your intended use is not permitted by statutory regulation or exceeds the permitted use, you will need to obtain permission directly from the copyright holder. To view a copy of this licence, visit <http://creativecommons.org/licenses/by/4.0/>.

References

- Abouzeid RE, Owda ME, Dacrory S (2022) Effective adsorption of cationic methylene blue dye on cellulose nanofiber/graphene oxide/silica nanocomposite: kinetics and equilibrium. *J Appl Polym Sci* 139(25):e52377. <https://doi.org/10.1002/app.52377>
- Adetayo A, Runsewe D (2019) Synthesis and fabrication of graphene and graphene oxide: a review. *Open J Compos Mater* 9(02):207
- Agarwal V, Zetterlund PB (2021) Strategies for reduction of graphene oxide – a comprehensive review. *Chem Eng J* 405:127018. <https://doi.org/10.1016/j.cej.2020.127018>
- Akindoyo JO, Ismail NH, Mariatti M (2019) Performance of poly(vinyl alcohol) nanocomposite reinforced with hybrid TEMPO mediated cellulose-graphene filler. *Polym Testing* 80:106140. <https://doi.org/10.1016/j.polymertesting.2019.106140>
- Al-Arjan WS, Khan MU, Almutairi HH, Alharbi SM, Razak SI (2022) pH-responsive PVA/BC-f-GO dressing materials for burn and chronic wound healing with curcumin release kinetics. *Polymers (Basel)* 14:1949
- Al-Shemy MT, Al-Sayed A, Dacrory S (2022) Fabrication of sodium alginate/graphene oxide/nanocrystalline cellulose scaffold for methylene blue adsorption: kinetics and thermodynamics study. *Sep Purif Technol* 290:120825. <https://doi.org/10.1016/j.seppur.2022.120825>
- Aly AA, Ahmed MK (2021) Nanofibers of cellulose acetate containing ZnO nanoparticles/graphene oxide for wound healing applications. *Int J Pharm* 598:120325. <https://doi.org/10.1016/j.ijpharm.2021.120325>
- Anglès MN, Dufresne A (2000) Plasticized starch/tunicin whiskers nanocomposites. 1. Structural analysis. *Macromolecules* 33(22):8344–8353. <https://doi.org/10.1021/ma0008701>
- Anirudhan TS, Deepa JR (2017) Nano-zinc oxide incorporated graphene oxide/nanocellulose composite for the adsorption and photo catalytic degradation of ciprofloxacin hydrochloride from aqueous solutions. *J Colloid Interface Sci* 490:343–356. <https://doi.org/10.1016/j.jcis.2016.11.042>
- Anirudhan TS, Deepa JR, Christa J (2016) Nanocellulose/nanobentonite composite anchored with multi-carboxyl functional groups as an adsorbent for the effective removal of Cobalt(II) from nuclear industry wastewater samples. *J Colloid Interface Sci* 467:307–320. <https://doi.org/10.1016/j.jcis.2016.01.023>
- Annu, Sharma S, Nitin A, Jain R (2020) Cellulose fabricated pencil graphite sensor for the quantification of hazardous herbicide atrazine. *Diam Relat Mater* 105:107788. <https://doi.org/10.1016/j.diamond.2020.107788>
- Ardekani HJ, Talaeipour M, Jouya Ardekani H, Hemmasi A, Bazyar B, Dufresne A (2022) Synthesis and characterization of nanocomposite films consisting of TEMPO-oxidized nanocellulose / Graphene oxide. *Nashrieh Shimi va Mohandesi Shimi Iran*. http://www.nsmi.ir/article_253842.html (Accessed on 20 August 2023)
- Ayissi Eyebe G, Bideau B, Boubekeur N, Loranger É, Domingue F (2017) Environmentally-friendly cellulose nanofibre sheets for humidity sensing in microwave frequencies. *Sens Actuators, B Chem* 245:484–492. <https://doi.org/10.1016/j.snb.2017.01.130>
- Azarniya A, Eslahi N, Mahmoudi N, Simchi A (2016) Effect of graphene oxide nanosheets on the physico-mechanical properties of chitosan/bacterial cellulose nanofibrous composites. *Compos A Appl Sci Manuf* 85:113–122. <https://doi.org/10.1016/j.compositesa.2016.03.011>
- Barbash VA, Yaschenko OV, Alushkin SV, Kondratyuk AS, Posudievsky OY, Koshechko VG (2016) The effect of mechanochemical treatment of the cellulose on characteristics of nanocellulose films. *Nanoscale Res Lett* 11(1):410. <https://doi.org/10.1186/s11671-016-1632-1>
- Basu S, Bhattacharyya P (2012) Recent developments on graphene and graphene oxide based solid state gas sensors.

- Sens Actuators, *B Chem* 173:1–21. <https://doi.org/10.1016/j.snb.2012.07.092>
- Beltramino F, Blanca Roncero M, Vidal T, Valls C (2018) A novel enzymatic approach to nanocrystalline cellulose preparation. *Carbohydr Polym* 189:39–47. <https://doi.org/10.1016/j.carbpol.2018.02.015>
- Bettaieb F, Khiari R, Hassan ML, Belgacem MN, Bras J, Dufresne A et al (2015) Preparation and characterization of new cellulose nanocrystals from marine biomass *Posidonia oceanica*. *Ind Crops Prod* 72:175–182. <https://doi.org/10.1016/j.indcrop.2014.12.038>
- Biswas MC, Jony B, Nandy PK, Chowdhury RA, Halder S, Kumar D et al (2022) Recent advancement of biopolymers and their potential biomedical applications. *J Polym Environ* 30(1):51–74. <https://doi.org/10.1007/s10924-021-02199-y>
- Boufi S (2017) 6 - Agricultural crop residue as a source for the production of cellulose nanofibrils. In Jawaid M, Boufi S, AKHPS (Eds), *Cellulose-reinforced nanofibre composites*. Woodhead Publishing, pp 129–152. <https://doi.org/10.1016/B978-0-08-100957-4.00006-1>
- Boufi S, Chaker A (2016) Easy production of cellulose nanofibrils from corn stalk by a conventional high speed blender. *Ind Crops Prod* 93:39–47. <https://doi.org/10.1016/j.indcrop.2016.05.030>
- Brakat A, Zhu H (2021) Nanocellulose-graphene hybrids: advanced functional materials as multifunctional sensing platform. *Nano-Micro Lett* 13(1):94. <https://doi.org/10.1007/s40820-021-00627-1>
- Burrs SL, Bhargava M, Sidhu R, Kiernan-Lewis J, Gomes C, Claussen JC et al (2016) A paper based graphene-nanocauliflower hybrid composite for point of care biosensing. *Biosens Bioelectron* 85:479–487. <https://doi.org/10.1016/j.bios.2016.05.037>
- Campano C, Miranda R, Merayo N, Negro C, Blanco A (2017) Direct production of cellulose nanocrystals from old newspapers and recycled newsprint. *Carbohydr Polym* 173:489–496. <https://doi.org/10.1016/j.carbpol.2017.05.073>
- Cao S, Li Q, Zhang S, Liu K, Yang Y, Chen J (2022) Oxidized bacterial cellulose reinforced nanocomposite scaffolds for bone repair. *Colloids Surf, B* 211:112316. <https://doi.org/10.1016/j.colsurfb.2021.112316>
- Chen W, Yan L (2011) In situ self-assembly of mild chemical reduction graphene for three-dimensional architectures. *Nanoscale* 3(8):3132–3137. <https://doi.org/10.1039/C1NR10355E>
- Chen C, Zhang T, Zhang Q, Chen X, Zhu C, Xu Y et al (2016a) Biointerface by cell growth on graphene oxide doped bacterial cellulose/poly(3,4-ethylenedioxythiophene) nanofibers. *ACS Appl Mater Interfaces* 8(16):10183–10192. <https://doi.org/10.1021/acsami.6b01243>
- Chen YW, Lee HV, Juan JC, Phang S-M (2016b) Production of new cellulose nanomaterial from red algae marine biomass *Gelidium elegans*. *Carbohydr Polym* 151:1210–1219. <https://doi.org/10.1016/j.carbpol.2016.06.083>
- Chen XY, Low HR, Loi XY, Merel L, MohdCairul Iqbal MA (2019) Fabrication and evaluation of bacterial nanocellulose/poly(acrylic acid)/graphene oxide composite hydrogel: characterizations and biocompatibility studies for wound dressing. *J Biomed Mater Res Part B: Appl Biomater* 107(6):2140–2151. <https://doi.org/10.1002/jbm.b.34309>
- Cong H-P, Wang P, Yu S-H (2013) Stretchable and self-healing graphene oxide-polymer composite hydrogels: a dual-network design. *Chem Mater* 25(16):3357–3362. <https://doi.org/10.1021/cm401919c>
- da Silva PMM, Camparotto NG, Figueiredo Neves T, Mastelaro VR, Nunes B, Siqueira Franco Picone C et al (2021) Instantaneous adsorption and synergic effect in simultaneous removal of complex dyes through nanocellulose/graphene oxide nanocomposites: batch, fixed-bed experiments and mechanism. *Environ Nanotechnol Monit Manag* 16:100584. <https://doi.org/10.1016/j.enmm.2021.100584>
- Dacroy S, Saeed AM, Abouzeid RE (2022) A novel ammonia sensor based on cellulose/graphene oxide functionalized with ethylenediamine. *Express Polym Lett* 16:786–797. <https://doi.org/10.3144/expresspolymlett.2022.58>
- Daniel WH, Abdul Majid Z, Mohd Muhid MN, Triwahyono S, Bakar MB, Ramli Z (2015) The reuse of wastewater for the extraction of cellulose nanocrystals. *Carbohydr Polym* 118:165–169. <https://doi.org/10.1016/j.carbpol.2014.10.072>
- Daniyal WMEMM, Fen YW, Abdullah J, Sadrolhosseini AR, Saleviter S, Omar NAS (2018a) Exploration of surface plasmon resonance for sensing copper ion based on nanocrystalline cellulose-modified thin film. *Opt Express* 26(26):34880–34893. <https://doi.org/10.1364/OE.26.034880>
- Daniyal WMEMM, Fen YW, Abdullah J, Saleviter S, Sheh Omar NA (2018b) Preparation and characterization of hexadecyltrimethylammonium bromide modified nanocrystalline cellulose/graphene oxide composite thin film and its potential in sensing copper ion using surface plasmon resonance technique. *Optik* 173:71–77. <https://doi.org/10.1016/j.ijleo.2018.08.014>
- Daniyal WMEMM, Fen YW, Abdullah J, Hashim HS, Fauzi NIM, Chanlek N et al (2020) X-ray photoelectron study on gold/nanocrystalline cellulose-graphene oxide thin film as surface plasmon resonance active layer for metal ion detection. *Thin Solid Films* 713:138340. <https://doi.org/10.1016/j.tsf.2020.138340>
- De Souza Lima MM, Wong JT, Paillet M, Borsali R, Pecora R (2003) Translational and rotational dynamics of Rodlike cellulose whiskers. *Langmuir* 19(1):24–29. <https://doi.org/10.1021/la020475z>
- Dogra I, Kumar BR, Etika KC, Chavali M, Khalifa AS, Gharib AF et al (2022) Environmentally friendly low-cost graphene oxide-cellulose nanocomposite filter for dye removal from water. *J King Saud Univ - Sci* 34(5):102122. <https://doi.org/10.1016/j.jksus.2022.102122>
- Du H, Parit M, Wu M, Che X, Wang Y, Zhang M et al (2020) Sustainable valorization of paper mill sludge into cellulose nanofibrils and cellulose nanopaper. *J Hazard Mater* 400:123106. <https://doi.org/10.1016/j.jhazmat.2020.123106>
- Dunlop MJ, Acharya B, Bissessur R (2018) Isolation of nanocrystalline cellulose from tunicates. *J Environ Chem Eng* 6(4):4408–4412. <https://doi.org/10.1016/j.jece.2018.06.056>
- Eigler S, Hirsch A (2014) Chemistry with graphene and graphene oxide—challenges for synthetic chemists. *Angew*

- Chem Int Ed 53(30):7720–7738. <https://doi.org/10.1002/anie.201402780>
- El Achaby M, Kassab Z, Aboulkas A, Gaillard C, Barakat A (2018) Reuse of red algae waste for the production of cellulose nanocrystals and its application in polymer nanocomposites. *Int J Biol Macromol* 106:681–691. <https://doi.org/10.1016/j.ijbiomac.2017.08.067>
- Espinosa E, Sánchez R, González Z, Domínguez-Robles J, Ferrari B, Rodríguez A (2017) Rapidly growing vegetables as new sources for lignocellulose nanofibre isolation: physicochemical, thermal and rheological characterisation. *Carbohydr Polym* 175:27–37. <https://doi.org/10.1016/j.carbpol.2017.07.055>
- Fan Y, Ma W, Han D, Gan S, Dong X, Niu L (2015) Convenient recycling of 3D AgX/graphene aerogels (X = Br, Cl) for efficient photocatalytic degradation of water pollutants. *Adv Mater* 27(25):3767–3773. <https://doi.org/10.1002/adma.201500391>
- Fattahi Meyabadi T, Dadashian F, Mir Mohamad Sadeghi G, Ebrahimi Zanjani Asl H (2014) Spherical cellulose nanoparticles preparation from waste cotton using a green method. *Powder Technol* 261:232–240. <https://doi.org/10.1016/j.powtec.2014.04.039>
- Flauzino Neto WP, Silvério HA, Dantas NO, Pasquini D (2013) Extraction and characterization of cellulose nanocrystals from agro-industrial residue – soy hulls. *Ind Crops Prod* 42:480–488. <https://doi.org/10.1016/j.indcrop.2012.06.041>
- Foster EJ, Moon RJ, Agarwal UP, Bortner MJ, Bras J, Camarero-Espinosa S et al (2018) Current characterization methods for cellulose nanomaterials. *Chem Soc Rev* 47(8):2609–2679. <https://doi.org/10.1039/C6CS00895J>
- French AD (2014) Idealized powder diffraction patterns for cellulose polymorphs. *Cellulose* 21(2):885–896. <https://doi.org/10.1007/s10570-013-0030-4>
- Gabryś T, Fryczkowska B, Fabia J, Biniś D (2022) Preparation of an active dressing by in situ biosynthesis of a bacterial cellulose-graphene oxide composite. *Polymers* 14:2864
- Garcia de Rodriguez NL, Thielemans W, Dufresne A (2006) Sisal cellulose whiskers reinforced polyvinyl acetate nanocomposites. *Cellulose* 13(3):261–270. <https://doi.org/10.1007/s10570-005-9039-7>
- Ghaee A, Bagheri-Khoulanjani S, Amir Afshar H, Bogheiri H (2019) Biomimetic nanocomposite scaffolds based on surface modified PCL-nanofibers containing curcumin embedded in chitosan/gelatin for skin regeneration. *Compos B Eng* 177:107339. <https://doi.org/10.1016/j.compositesb.2019.107339>
- Gu H, Gao C, Zhou X, Du A, Naik N, Guo Z (2021) Nanocellulose nanocomposite aerogel towards efficient oil and organic solvent adsorption. *Adv Compos Hybrid Mater* 4(3):459–468. <https://doi.org/10.1007/s42114-021-00289-y>
- Guan F, Chen S, Sheng N, Chen Y, Yao J, Pei Q et al (2019) Mechanically robust reduced graphene oxide/bacterial cellulose film obtained via biosynthesis for flexible supercapacitor. *Chem Eng J* 360:829–837. <https://doi.org/10.1016/j.cej.2018.11.202>
- Hao D, Liu J, Sun H, Fu B, Liu J, Zhou J (2022) Integration of g-C₃N₄ into cellulose/graphene oxide foams for efficient photocatalytic Cr(VI) reduction. *J Phys Chem Solids* 169:110813. <https://doi.org/10.1016/j.jpcs.2022.110813>
- Hashem AH, Hasanin M, Kamel S, Dacrory S (2022) A new approach for antimicrobial and antiviral activities of bio-compatible nanocomposite based on cellulose, amino acid and graphene oxide. *Colloids Surf, B* 209:112172. <https://doi.org/10.1016/j.colsurfb.2021.112172>
- Hekimoğlu G, Çakır E, Sari A, Gencil O, Tyagi VV, Sharma RK (2023) Shape stabilized microcrystalline cellulose/methyl stearate/graphene nanoplatelet composite with enriched thermal conductivity and thermal energy storage/release performance. *Cellulose* 30(16):10199–10214. <https://doi.org/10.1007/s10570-023-05526-9>
- Hernández-Becerra E, Osorio M, Marín D, Gañán P, Pereira M, Builes D et al (2023) Isolation of cellulose microfibrils and nanofibers by mechanical fibrillation in a water-free solvent. *Cellulose* 30(8):4905–4923. <https://doi.org/10.1007/s10570-023-05162-3>
- Horta-Velázquez A, Morales-Narváez E (2022) Nanocellulose in wearable sensors. *Green Anal Chem* 1:100009. <https://doi.org/10.1016/j.greeac.2022.100009>
- Huang G, Hou C, Shao Y, Wang H, Zhang Q, Li Y et al (2014) Highly strong and elastic graphene fibres prepared from universal graphene oxide precursors. *Sci Rep* 4(1):4248. <https://doi.org/10.1038/srep04248>
- Hui Y, Xie W, Gu H (2021) Reduced graphene oxide/nanocellulose/amino-multiwalled carbon nanotubes nanocomposite aerogel for excellent oil adsorption (journal article). *ES Food Agrofor* 5:38–44. <https://doi.org/10.30919/esfaf531>
- Hussain A, Li J, Wang J, Xue F, Chen Y, Bin Aftab T et al (2018) Hybrid monolith of graphene/TEMPO-oxidized cellulose nanofiber as mechanically robust, highly functional, and recyclable adsorbent of methylene blue dye. *J Nanomater* 2018:5963982. <https://doi.org/10.1155/2018/5963982>
- Hwang S, Walker CC, Ozcan S, Tekinalp H, Han Y, Gardner DJ (2024) Characterization of spray dried cellulose nanofibrils produced by a disk refining process at different fineness levels. *Cellulose* 31(1):263–277. <https://doi.org/10.1007/s10570-023-05613-x>
- Ifuku S (2014) Chitin and chitosan nanofibers: preparation and chemical modifications. *Molecules* 19(11). <https://doi.org/10.3390/molecules191118367>
- Iijima S, Ichihashi T (1993) Single-shell carbon nanotubes of 1-nm diameter. *Nature* 363(6430):603–605. <https://doi.org/10.1038/363603a0>
- Ikram R, Jan BM, Ahmad W (2020) An overview of industrial scalable production of graphene oxide and analytical approaches for synthesis and characterization. *J Market Res* 9(5):11587–11610. <https://doi.org/10.1016/j.jmrt.2020.08.050>
- Ikram M, Rasheed F, Haider A, Naz S, Ul-Hamid A, Shahzadi A et al (2022) Photocatalytic and antibacterial activity of graphene oxide/cellulose-doped TiO₂ quantum dots: in silico molecular docking studies. *Nanoscale Adv* 4(18):3764–3776. <https://doi.org/10.1039/D2NA00383J>
- Javadi A, Zheng Q, Payen F, Javadi A, Altin Y, Cai Z et al (2013) Polyvinyl alcohol-cellulose nanofibrils-graphene oxide hybrid organic aerogels. *ACS Appl Mater*

- Interfaces 5(13):5969–5975. <https://doi.org/10.1021/am400171y>
- Ji C-C, Xu M-W, Bao S-J, Cai C-J, Lu Z-J, Chai H et al (2013) Self-assembly of three-dimensional interconnected graphene-based aerogels and its application in supercapacitors. *J Colloid Interface Sci* 407:416–424. <https://doi.org/10.1016/j.jcis.2013.06.054>
- Jia Y, Hu C, Shi P, Xu Q, Zhu W, Liu R (2020) Effects of cellulose nanofibrils/graphene oxide hybrid nanofiller in PVA nanocomposites. *Int J Biol Macromol* 161:223–230. <https://doi.org/10.1016/j.ijbiomac.2020.06.013>
- Jiang Q, Ghim D, Cao S, Tadepalli S, Liu K-K, Kwon H et al (2019) Photothermally active reduced graphene oxide/bacterial nanocellulose composites as biofouling-resistant ultrafiltration membranes. *Environ Sci Technol* 53(1):412–421. <https://doi.org/10.1021/acs.est.8b02772>
- Jiao D, Song N, Ding P, Shi L (2022) Enhanced thermal conductivity in oriented cellulose nanofibril/graphene composites via interfacial engineering. *Compos Commun* 31:101101. <https://doi.org/10.1016/j.coco.2022.101101>
- Jin L, Zeng Z, Kuddannaya S, Wu D, Zhang Y, Wang Z (2016) Biocompatible, free-standing film composed of bacterial cellulose nanofibers-graphene composite. *ACS Appl Mater Interfaces* 8(1):1011–1018. <https://doi.org/10.1021/acsami.5b11241>
- Kafy A, Akther A, Shishir MIR, Kim HC, Yun Y, Kim J (2016) Cellulose nanocrystal/graphene oxide composite film as humidity sensor. *Sens Actuators, A* 247:221–226. <https://doi.org/10.1016/j.sna.2016.05.045>
- Khamrai M, Banerjee SL, Paul S, Ghosh AK, Sarkar P, Kundu PP (2019) A mussel mimetic, bioadhesive, antimicrobial patch based on dopamine-modified bacterial cellulose/rGO/Ag NPs: a green approach toward wound-healing applications. *ACS Sustain Chem Eng* 7(14):12083–12097. <https://doi.org/10.1021/acssuschemeng.9b01163>
- Khan S, Ul-Islam M, Ullah MW, Zhu Y, Narayanan KB, Han SS et al (2022) Fabrication strategies and biomedical applications of three-dimensional bacterial cellulose-based scaffolds: a review. *Int J Biol Macromol* 209:9–30. <https://doi.org/10.1016/j.ijbiomac.2022.03.191>
- Khan MUA, Stojanović GM, Hassan R, Anand TJS, Al-Ejji M, Hasan A (2023) Role of graphene oxide in bacterial cellulose–gelatin hydrogels for wound dressing applications. *ACS Omega* 8(18):15909–15919. <https://doi.org/10.1021/acsomega.2c07279>
- Kim HJ, Park SH (2022) Reinforced tensile strength and wettability of nanofibrous electrospun cellulose acetate by coating with waterborne polyurethane and graphene oxide. *J Eng Fibers Fabr* 17:15589250221127352. <https://doi.org/10.1177/15589250221127353>
- Kim S-S, Jeon J-H, Kim H-I, Kee CD, Oh I-K (2015) High-fidelity bioelectronic muscular actuator based on graphene-mediated and TEMPO-oxidized bacterial cellulose. *Adv Func Mater* 25(23):3560–3570. <https://doi.org/10.1002/adfm.201500673>
- Kim HC, Panicker PS, Kim D, Adil S, Kim J (2021) High-strength cellulose nanofiber/graphene oxide hybrid filament made by continuous processing and its humidity monitoring. *Sci Rep* 11(1):13611. <https://doi.org/10.1038/s41598-021-93209-5>
- Lee C, Wei X, Kysar Jeffrey W, Hone J (2008) Measurement of the elastic properties and intrinsic strength of monolayer graphene. *Science* 321(5887):385–388. <https://doi.org/10.1126/science.1157996>
- Lefatshe K, Muiva CM, Kebaabetswe LP (2017) Extraction of nanocellulose and in-situ casting of ZnO/cellulose nanocomposite with enhanced photocatalytic and antibacterial activity. *Carbohydr Polym* 164:301–308. <https://doi.org/10.1016/j.carbpol.2017.02.020>
- Li Y, Du Q, Liu T, Peng X, Wang J, Sun J et al (2013) Comparative study of methylene blue dye adsorption onto activated carbon, graphene oxide, and carbon nanotubes. *Chem Eng Res Des* 91(2):361–368. <https://doi.org/10.1016/j.cherd.2012.07.007>
- Li Y, Zhu H, Zhu S, Wan J, Liu Z, Vaaland O et al (2015) Hybridizing wood cellulose and graphene oxide toward high-performance fibers. *NPG Asia Mater* 7(1):e150–e150. <https://doi.org/10.1038/am.2014.111>
- Li X, Shao C, Zhuo B, Yang S, Zhu Z, Su C et al (2019) The use of nanofibrillated cellulose to fabricate a homogeneous and flexible graphene-based electric heating membrane. *Int J Biol Macromol* 139:1103–1116. <https://doi.org/10.1016/j.ijbiomac.2019.08.081>
- Li B, Chen Y, Han Y, Cao X, Luo Z (2022) Tough, highly resilient and conductive nanocomposite hydrogels reinforced with surface-grafted cellulose nanocrystals and reduced graphene oxide for flexible strain sensors. *Colloids Surf, A* 648:129341. <https://doi.org/10.1016/j.colsurfa.2022.129341>
- Li J, Meng L, Chen J, Chen X, Wang Y, Xiao Z et al (2023) Encapsulation of polyethylene glycol in cellulose-based porous capsules for latent heat storage and light-to-thermal conversion. *Front Chem Sci Eng* 17(8):1038–1050. <https://doi.org/10.1007/s11705-022-2279-3>
- Liang Y, Wei Z, Wang H-E, Flores M, Wang R, Zhang X (2022) Flexible and freestanding PANI: PSS/CNF nanopaper electrodes with enhanced electrochemical performance for supercapacitors. *J Power Sources* 548:232071. <https://doi.org/10.1016/j.jpowsour.2022.232071>
- Liu P, Zhu C, Mathew AP (2019) Mechanically robust high flux graphene oxide - nanocellulose membranes for dye removal from water. *J Hazard Mater* 371:484–493. <https://doi.org/10.1016/j.jhazmat.2019.03.009>
- Liu Y, Fan Q, Huo Y, Liu C, Li B, Li Y (2020) Construction of a mesoporous polydopamine@GO/cellulose nanofibril composite hydrogel with an encapsulation structure for controllable drug release and toxicity shielding. *ACS Appl Mater Interfaces* 12(51):57410–57420. <https://doi.org/10.1021/acsami.0c15465>
- Liu X, Ma Y, Zhang X, Huang J (2021) Cellulose nanocrystal reinforced conductive nanocomposite hydrogel with fast self-healing and self-adhesive properties for human motion sensing. *Colloids Surf, A* 613:126076. <https://doi.org/10.1016/j.colsurfa.2020.126076>
- Lu P, Hsieh Y-L (2010) Preparation and properties of cellulose nanocrystals: rods, spheres, and network. *Carbohydr Polym* 82(2):329–336. <https://doi.org/10.1016/j.carbpol.2010.04.073>
- Lu Y, Yue Y, Ding Q, Mei C, Xu X, Wu Q et al (2021) Self-recovery, fatigue-resistant, and multifunctional sensor assembled by a nanocellulose/carbon nanotube nanocomplex-mediated

- hydrogel. *ACS Appl Mater Interfaces* 13(42):50281–50297. <https://doi.org/10.1021/acsami.1c16828>
- Luo H, Ao H, Li G, Li W, Xiong G, Zhu Y et al (2017) Bacterial cellulose/graphene oxide nanocomposite as a novel drug delivery system. *Curr Appl Phys* 17(2):249–254. <https://doi.org/10.1016/j.cap.2016.12.001>
- Luo H, Dong J, Yao F, Yang Z, Li W, Wang J et al (2018) Layer-by-layer assembled bacterial cellulose/graphene oxide hydrogels with extremely enhanced mechanical properties. *Nano-Micro Letters* 10(3):42. <https://doi.org/10.1007/s40820-018-0195-3>
- Luo H, Ao H, Peng M, Yao F, Yang Z, Wan Y (2019a) Effect of highly dispersed graphene and graphene oxide in 3D nanofibrous bacterial cellulose scaffold on cell responses: a comparative study. *Mater Chem Phys* 235:121774. <https://doi.org/10.1016/j.matchemphys.2019.121774>
- Luo H, Xie J, Xiong L, Zhu Y, Yang Z, Wan Y (2019b) Fabrication of flexible, ultra-strong, and highly conductive bacterial cellulose-based paper by engineering dispersion of graphene nanosheets. *Compos B Eng* 162:484–490. <https://doi.org/10.1016/j.compositesb.2019.01.027>
- Marimuthu TS, Atmakuru R (2015) Isolation and characterization of cellulose nanofibers from the aquatic weed water hyacinth: *eichhornia crassipes*. In Pandey JK, Takagi H, Nakagaito AN, Kim H-J (Eds.), *Handbook of polymer nanocomposites. processing, performance and application: volume c: polymer nanocomposites of cellulose nanoparticles*. Springer Berlin Heidelberg, Berlin, Heidelberg, pp 37–46. https://doi.org/10.1007/978-3-642-45232-1_55
- Mautner A, Maples HA, Kobkeathawin T, Kokol V, Karim Z, Li K et al (2016) Phosphorylated nanocellulose papers for copper adsorption from aqueous solutions. *Int J Environ Sci Technol* 13(8):1861–1872. <https://doi.org/10.1007/s13762-016-1026-z>
- Migliorini FL, Teodoro KBR, Scagion VP, dos Santos DM, Fonseca FJ, Mattoso LHC et al (2019) Tuning the electrical properties of electrospun nanofibers with hybrid nanomaterials for detecting isoborneol in water using an electronic tongue. *Surfaces* 2(2):432. <https://doi.org/10.3390/surfaces2020031>
- Min P, Liu J, Li X, An F, Liu P, Shen Y et al (2018) Thermally conductive phase change composites featuring anisotropic graphene aerogels for real-time and fast-charging solar-thermal energy conversion. *Adv Func Mater* 28(51):1805365. <https://doi.org/10.1002/adfm.201805365>
- Mo M, Chen C, Gao H, Chen M, Li D (2018) Wet-spinning assembly of cellulose nanofibers reinforced graphene/polypyrrole microfibers for high performance fiber-shaped supercapacitors. *Electrochim Acta* 269:11–20. <https://doi.org/10.1016/j.electacta.2018.02.118>
- Mochane MJ, Luyt AS (2012) Preparation and properties of polystyrene encapsulated paraffin wax as possible phase change material in a polypropylene matrix. *Thermochim Acta* 544:63–70. <https://doi.org/10.1016/j.tca.2012.06.017>
- Mokhena TC, John MJ (2020a) Cellulose nanomaterials: new generation materials for solving global issues. *Cellulose* 27(3):1149–1194. <https://doi.org/10.1007/s10570-019-02889-w>
- Mokhena TC, John MJ (2020b) Esterified cellulose nanofibers from saw dust using vegetable oil. *Int J Biol Macromol* 148:1109–1117. <https://doi.org/10.1016/j.ijbiomac.2020.01.278>
- Mokhena TC, Luyt AS (2014) Investigation of polyethylene/sisal whiskers nanocomposites prepared under different conditions. *Polym Compos* 35(11):2221–2233. <https://doi.org/10.1002/pc.22887>
- Mokhena TC, Luyt AS (2017) Development of multifunctional nano/ultrafiltration membrane based on a chitosan thin film on alginate electrospun nanofibres. *J Clean Prod* 156:470–479. <https://doi.org/10.1016/j.jclepro.2017.04.073>
- Mokhena TC, Matabola KP, Mokhothu TH, Mtibe A, Mochane MJ, Ndlovu G et al (2022) Electrospun carbon nanofibres: preparation, characterization and application for adsorption of pollutants from water and air. *Sep Purif Technol* 288:120666. <https://doi.org/10.1016/j.seppur.2022.120666>
- Montes S, Carrasco PM, Ruiz V, Cabañero G, Grande HJ, Labidi J et al (2015) Synergistic reinforcement of poly(vinyl alcohol) nanocomposites with cellulose nanocrystal-stabilized graphene. *Compos Sci Technol* 117:26–31. <https://doi.org/10.1016/j.compscitech.2015.05.018>
- Mtibe A, Mokhothu TH, John MJ, Mokhena TC, Mochane MJ (2018) Chapter 8 - fabrication and characterization of various engineered nanomaterials. In Mustansar Hussain C (Ed.), *handbook of nanomaterials for industrial applications*. Elsevier, pp 151–171. <https://doi.org/10.1016/B978-0-12-813351-4.00009-2>
- Neibolts N, Platnieks O, Gaidukovs S, Barkane A, Thakur VK, Filipova I et al (2020) Needle-free electrospinning of nanofibrillated cellulose and graphene nanoplatelets based sustainable poly (butylene succinate) nanofibers. *Mater Today Chem* 17:100301. <https://doi.org/10.1016/j.mtchem.2020.100301>
- Nguyen VT, Ha LQ, Nguyen TDL, Ly PH, Nguyen DM, Hoang D (2022) Nanocellulose and graphene oxide aerogels for adsorption and removal methylene blue from an aqueous environment. *ACS Omega* 7(1):1003–1013. <https://doi.org/10.1021/acsomega.1c05586>
- Niamsap T, Lam NT, Sukyai P (2019) Production of hydroxyapatite-bacterial nanocellulose scaffold with assist of cellulose nanocrystals. *Carbohydr Polym* 205:159–166. <https://doi.org/10.1016/j.carbpol.2018.10.034>
- Nishiyama Y, Langan P, Chanzy H (2002) Crystal structure and hydrogen-bonding system in cellulose I β from synchrotron x-ray and neutron fiber diffraction. *J Am Chem Soc* 124(31):9074–9082. <https://doi.org/10.1021/ja0257319>
- Nishiyama Y, Sugiyama J, Chanzy H, Langan P (2003) Crystal structure and hydrogen bonding system in cellulose I α from synchrotron x-ray and neutron fiber diffraction. *J Am Chem Soc* 125(47):14300–14306. <https://doi.org/10.1021/ja037055w>
- Nizam PA, Arumughan V, Baby A, Sunil MA, Pasquini D, Nzihou A et al (2020) Mechanically robust antibacterial nanopapers through mixed dimensional assembly for anionic dye removal. *J Polym Environ* 28(4):1279–1291. <https://doi.org/10.1007/s10924-020-01681-3>
- Oprea M, Voicu SI (2020) Cellulose composites with graphene for tissue engineering applications. *Materials* 13:5347

- Oun AA, Shankar S, Rhim J-W (2020) Multifunctional nano-cellulose/metal and metal oxide nanoparticle hybrid nanomaterials. *Crit Rev Food Sci Nutr* 60(3):435–460. <https://doi.org/10.1080/10408398.2018.1536966>
- Pal N, Dubey P, Gopinath P, Pal K (2017) Combined effect of cellulose nanocrystal and reduced graphene oxide into poly-lactic acid matrix nanocomposite as a scaffold and its anti-bacterial activity. *Int J Biol Macromol* 95:94–105. <https://doi.org/10.1016/j.ijbiomac.2016.11.041>
- Pal N, Banerjee S, Roy P, Pal K (2019a) Melt-blending of unmodified and modified cellulose nanocrystals with reduced graphene oxide into PLA matrix for biomedical application. *Polym Adv Technol* 30(12):3049–3060. <https://doi.org/10.1002/pat.4736>
- Pal N, Banerjee S, Roy P, Pal K (2019b) Reduced graphene oxide and PEG-grafted TEMPO-oxidized cellulose nanocrystal reinforced poly-lactic acid nanocomposite film for biomedical application. *Mater Sci Eng, C* 104:109956. <https://doi.org/10.1016/j.msec.2019.109956>
- Passornraprasit N, Siripongpreda T, Ninlapruk S, Rodthongkum N, Potiyaraj P (2022) γ -Irradiation crosslinking of graphene oxide/cellulose nanofiber/poly (acrylic acid) hydrogel as a urea sensing patch. *Int J Biol Macromol* 213:1037–1046. <https://doi.org/10.1016/j.ijbiomac.2022.06.053>
- Pennells J, Godwin ID, Amiralian N, Martin DJ (2020) Trends in the production of cellulose nanofibers from non-wood sources. *Cellulose* 27(2):575–593. <https://doi.org/10.1007/s10570-019-02828-9>
- Peresin MS, Habibi Y, Zoppe JO, Pawlak JJ, Rojas OJ (2010) Nanofiber composites of polyvinyl alcohol and cellulose nanocrystals: manufacture and characterization. *Biomacromol* 11(3):674–681. <https://doi.org/10.1021/bm901254n>
- Portela R, Leal CR, Almeida PL, Sobral RG (2019) Bacterial cellulose: a versatile biopolymer for wound dressing applications. *Microb Biotechnol* 12(4):586–610. <https://doi.org/10.1111/1751-7915.13392>
- Pottathara YB, Bobnar V, Finšgar M, Grohens Y, Thomas S, Kokol V (2018) Cellulose nanofibrils-reduced graphene oxide xerogels and cryogels for dielectric and electrochemical storage applications. *Polymer* 147:260–270. <https://doi.org/10.1016/j.polymer.2018.06.005>
- Prakash J, Venkataprasanna KS, Bharath G, Banat F, Niranjan R, Venkatasubbu GD (2021) In-vitro evaluation of electrospun cellulose acetate nanofiber containing graphene oxide/TiO₂/curcumin for wound healing application. *Colloids Surf, A* 627:127166. <https://doi.org/10.1016/j.colsurfa.2021.127166>
- Prasad Reddy J, Rhim J-W (2014) Isolation and characterization of cellulose nanocrystals from garlic skin. *Mater Lett* 129:20–23. <https://doi.org/10.1016/j.matlet.2014.05.019>
- Putz KW, Compton OC, Segar C, An Z, Nguyen ST, Brinson LC (2011) Evolution of order during vacuum-assisted self-assembly of graphene oxide paper and associated polymer nanocomposites. *ACS Nano* 5(8):6601–6609. <https://doi.org/10.1021/nn202040c>
- Qian Y, Ismail IM, Stein A (2014) Ultralight, high-surface-area, multifunctional graphene-based aerogels from self-assembly of graphene oxide and resol. *Carbon* 68:221–231. <https://doi.org/10.1016/j.carbon.2013.10.082>
- Qiu J, Li M, Ding M, Yao J (2022) Cellulose tailored semiconductors for advanced photocatalysis. *Renew Sustain Energy Rev* 154:111820. <https://doi.org/10.1016/j.rser.2021.111820>
- Qiu S, Liao D, Wang Z, Yuan Y, You Q, Chen Y et al (2024) Pickering emulsion for multifunctional cellulose/graphene oxide/paraffin wax-derived carbon aerogel film with photothermal and Joule heating performance for pressure sensors. *Ceram Int*. <https://doi.org/10.1016/j.ceramint.2024.01.377>
- Ramani D, Sastry TP (2014) Bacterial cellulose-reinforced hydroxyapatite functionalized graphene oxide: a potential osteoinductive composite. *Cellulose* 21(5):3585–3595. <https://doi.org/10.1007/s10570-014-0313-4>
- Rashidian E, Babaeipour V, Chegeni A, Khodamoradi N, Omidi M (2021) Synthesis and characterization of bacterial cellulose/graphene oxide nano-biocomposites. *Polym Compos* 42(9):4698–4706. <https://doi.org/10.1002/pc.26179>
- Ren F, Tan W, Duan Q, Jin Y, Pei L, Ren P et al (2019) Ultra-low gas permeable cellulose nanofiber nanocomposite films filled with highly oriented graphene oxide nanosheets induced by shear field. *Carbohydr Polym* 209:310–319. <https://doi.org/10.1016/j.carbpol.2019.01.040>
- Roman M, Winter WT (2004) Effect of sulfate groups from sulfuric acid hydrolysis on the thermal degradation behavior of bacterial cellulose. *Biomacromol* 5(5):1671–1677. <https://doi.org/10.1021/bm034519+>
- Roy N, Kannabiran K, Mukherjee A (2023) Integrated adsorption and photocatalytic degradation based removal of ciprofloxacin and sulfamethoxazole antibiotics using Fc@rGO-ZnO nanocomposite in aqueous systems. *Chemosphere* 333:138912. <https://doi.org/10.1016/j.chemosphere.2023.138912>
- Ruiz-Palomero C, Benítez-Martínez S, Soriano ML, Valcárcel M (2017) Fluorescent nanocellulosic hydrogels based on graphene quantum dots for sensing laccase. *Anal Chim Acta* 974:93–99. <https://doi.org/10.1016/j.aca.2017.04.018>
- Rwegasila E, Li L, Berglund LA, Mushi NE (2024) Strong nanostructured film and effective lead (II) removal by nitro-oxidized cellulose nanofibrils from banana rachis. *Cellulose*. <https://doi.org/10.1007/s10570-024-05749-4>
- Sadasivuni KK, Kafy A, Zhai L, Ko H-U, Mun S, Kim J (2015) Transparent and flexible cellulose nanocrystal/reduced graphene oxide film for proximity sensing. *Small* 11(8):994–1002. <https://doi.org/10.1002/sml.201402109>
- Sajab MS, Chia CH, Chan CH, Zakaria S, Kaco H, Chook SW et al (2016) Bifunctional graphene oxide–cellulose nanofibril aerogel loaded with Fe(III) for the removal of cationic dye via simultaneous adsorption and Fenton oxidation. *RSC Adv* 6(24):19819–19825. <https://doi.org/10.1039/C5RA26193G>
- Salleh A, Mustafa N, Teow YH, Fatimah MN, Khairudin FA, Ahmad I et al (2022) Dual-layered approach of ovine collagen-gelatin/cellulose hybrid biomatrix containing graphene oxide-silver nanoparticles for cutaneous wound healing: fabrication, physicochemical, cytotoxicity and antibacterial characterisation. *Biomedicines* 10(4):816
- Shao C, Zhu Z, Su C, Yang S, Yuan Q (2018) Thin electric heating membrane constructed with a three-dimensional

- nanofibrillated cellulose–graphene–graphene oxide system. *Materials* 11(9):1727. <https://www.mdpi.com/1996-1944/11/9/1727>
- Shende P, Pathan N (2021) Potential of carbohydrate-conjugated graphene assemblies in biomedical applications. *Carbohydr Polym* 255:117385. <https://doi.org/10.1016/j.carbpol.2020.117385>
- Shi L, Hong G, Chen C, Li X, Zhang H, Chai R et al (2023) Growth of spiral ganglion neurons induced by graphene oxide/oxidized bacterial cellulose composite hydrogel. *Carbohydr Polym* 311:120749. <https://doi.org/10.1016/j.carbpol.2023.120749>
- Shin SR, Zihlmann C, Akbari M, Assawes P, Cheung L, Zhang K et al (2016) Reduced graphene oxide–GelMA hybrid hydrogels as scaffolds for cardiac tissue engineering. *Small* 12(27):3677–3689. <https://doi.org/10.1002/sml.201600178>
- Si H, Luo H, Xiong G, Yang Z, Raman SR, Guo R et al (2014) One-step in situ biosynthesis of graphene oxide–bacterial cellulose nanocomposite hydrogels. *Macromol Rapid Commun* 35(19):1706–1711. <https://doi.org/10.1002/marc.201400239>
- Stanisic D, Cruz GCF, Elias LA, Tsukamoto J, Arns CW, Soares da Silva D et al (2022) High-resolution magic-angle spinning nmr spectroscopy for evaluation of cell shielding by virucidal composites based on biogenic silver nanoparticles, flexible cellulose nanofibers and graphene oxide (original research). *Front Bioeng Biotechnol* 10. <https://doi.org/10.3389/fbioe.2022.858156>
- Tang Z, Shen S, Zhuang J, Wang X (2010) Noble-metal-promoted three-dimensional macroassembly of single-layered graphene oxide. *Angew Chem Int Ed* 49(27):4603–4607. <https://doi.org/10.1002/anie.201000270>
- Tang Y, Shen X, Zhang J, Guo D, Kong F, Zhang N (2015) Extraction of cellulose nano-crystals from old corrugated container fiber using phosphoric acid and enzymatic hydrolysis followed by sonication. *Carbohydr Polym* 125:360–366. <https://doi.org/10.1016/j.carbpol.2015.02.063>
- Tarchoun AF, Trache D, Klapötke TM (2019) Microcrystalline cellulose from *Posidonia oceanica* brown algae: extraction and characterization. *Int J Biol Macromol* 138:837–845. <https://doi.org/10.1016/j.ijbiomac.2019.07.176>
- Teixeira RSS, da Silva ASA, Jang J-H, Kim H-W, Ishikawa K, Endo T et al (2015) Combining biomass wet disk milling and endoglucanase/ β -glucosidase hydrolysis for the production of cellulose nanocrystals. *Carbohydr Polym* 128:75–81. <https://doi.org/10.1016/j.carbpol.2015.03.087>
- Teo HL, Wahab RA (2020) Towards an eco-friendly deconstruction of agro-industrial biomass and preparation of renewable cellulose nanomaterials: a review. *Int J Biol Macromol* 161:1414–1430. <https://doi.org/10.1016/j.ijbiomac.2020.08.076>
- Teodoro KBR, Migliorini FL, Fature MHM, Correa DS (2019) Conductive electrospun nanofibers containing cellulose nanowhiskers and reduced graphene oxide for the electrochemical detection of mercury(II). *Carbohydr Polym* 207:747–754. <https://doi.org/10.1016/j.carbpol.2018.12.022>
- Teodoro KBR, Sanfelice RC, Migliorini FL, Pavinatto A, Fature MHM, Correa DS (2021) A review on the role and performance of cellulose nanomaterials in sensors. *ACS Sensors* 6(7):2473–2496. <https://doi.org/10.1021/acssensors.1c00473>
- ThiripuraSundari M, Ramesh A (2012) Isolation and characterization of cellulose nanofibers from the aquatic weed water hyacinth—*Eichhornia crassipes*. *Carbohydr Polym* 87(2):1701–1705. <https://doi.org/10.1016/j.carbpol.2011.09.076>
- Torres FG, Ccorahua R, Arroyo J, Troncoso OP (2019) Enhanced conductivity of bacterial cellulose films reinforced with NH₄-doped graphene oxide. *Polym-Plast Technol Mater* 58(14):1585–1595. <https://doi.org/10.1080/25740881.2018.1563135>
- Trache D, Tarchoun AF, Derradji M, Hamidon TS, Masruchin N, Brosse N et al (2020) Nanocellulose: from fundamentals to advanced applications (review). *Front Chem* 8. <https://doi.org/10.3389/fchem.2020.00392>
- Tsai J-L, Tu J-F (2010) Characterizing mechanical properties of graphite using molecular dynamics simulation. *Mater Des* 31(1):194–199. <https://doi.org/10.1016/j.matdes.2009.06.032>
- Uddin AJ, Araki J, Gotoh Y (2011) Characterization of the poly(vinyl alcohol)/cellulose whisker gel spun fibers. *Compos A Appl Sci Manuf* 42(7):741–747. <https://doi.org/10.1016/j.compositesa.2011.02.012>
- Urbina L, Eceiza A, Gabilondo N, Corcuera MÁ, Retegi A (2020) Tailoring the in situ conformation of bacterial cellulose–graphene oxide spherical nanocarriers. *Int J Biol Macromol* 163:1249–1260. <https://doi.org/10.1016/j.ijbiomac.2020.07.077>
- Valentini L, Cardinali M, Fortunati E, Torre L, Kenny JM (2013) A novel method to prepare conductive nanocrystalline cellulose/graphene oxide composite films. *Mater Lett* 105:4–7. <https://doi.org/10.1016/j.matlet.2013.04.034>
- Van Hai L, Zhai L, Kim HC, Kim JW, Choi ES, Kim J (2018) Cellulose nanofibers isolated by TEMPO-oxidation and aqueous counter collision methods. *Carbohydr Polym* 191:65–70. <https://doi.org/10.1016/j.carbpol.2018.03.008>
- Verma R, Nagendra HN, Kasthurirengan S, Shivaprakash NC, Behera U (2019) Thermal conductivity studies on activated carbon based cryopanel. *IOP Conf Ser: Mater Sci Eng* 502(1):012197. <https://doi.org/10.1088/1757-899X/502/1/012197>
- Wahid F, Huang L-H, Zhao X-Q, Li W-C, Wang Y-Y, Jia S-R et al (2021) Bacterial cellulose and its potential for biomedical applications. *Biotechnol Adv* 53:107856. <https://doi.org/10.1016/j.biotechadv.2021.107856>
- Walling B, Bharali P, Ramachandran D, Viswanathan K, Hazarika S, Dutta N et al (2023) In-situ biofabrication of bacterial nanocellulose (BNC)/graphene oxide (GO) nano-biocomposite and study of its cationic dyes adsorption properties. *Int J Biol Macromol* 251:126309. <https://doi.org/10.1016/j.ijbiomac.2023.126309>
- Wan C, Li J (2016) Incorporation of graphene nanosheets into cellulose aerogels: enhanced mechanical, thermal, and oil adsorption properties. *Appl Phys A* 122(2):105. <https://doi.org/10.1007/s00339-016-9641-6>
- Wang F, Drzal LT, Qin Y, Huang Z (2015) Multifunctional graphene nanoplatelets/cellulose nanocrystals composite paper. *Compos B Eng* 79:521–529. <https://doi.org/10.1016/j.compositesb.2015.04.031>

- Wang S, Yang L, Wang Q, Fan Y, Shang J, Qiu S et al (2018) Supramolecular self-assembly of layer-by-layer graphene film driven by the synergism of π - π and hydrogen bonding interaction. *J Photochem Photobiol, A* 355:249–255. <https://doi.org/10.1016/j.jphotochem.2017.09.023>
- Wang M, Chen Y, Qin Y, Wang T, Yang J, Xu F (2019) Compressible, fatigue resistant, and pressure-sensitive carbon aerogels developed with a facile method for sensors and electrodes. *ACS Sustain Chem Eng* 7(15):12726–12733. <https://doi.org/10.1021/acsschemeng.9b00814>
- Wang L, Li K, Copenhaver K, Mackay S, Lamm ME, Zhao X et al (2021a) Review on nonconventional fibrillation methods of producing cellulose nanofibrils and their applications. *Biomacromol* 22(10):4037–4059. <https://doi.org/10.1021/acs.biomac.1c00640>
- Wang Z, Song L, Wang Y, Zhang X-F, Yao J (2021b) Construction of a hybrid graphene oxide/nanofibrillated cellulose aerogel used for the efficient removal of methylene blue and tetracycline. *J Phys Chem Solids* 150:109839. <https://doi.org/10.1016/j.jpcs.2020.109839>
- Wang F, Huang D, Li Q, Wu Y, Yan B, Wu Z et al (2023) Highly electro-responsive ionic soft actuator based on graphene nanoplatelets-mediated functional carboxylated cellulose nanofibers. *Compos Sci Technol* 231:109845. <https://doi.org/10.1016/j.compscitech.2022.109845>
- Wei J, Gui S-H, Wu J-H, Xu D-D, Sun Y, Dong X-Y et al (2019) Nanocellulose-graphene oxide hybrid aerogel to water purification (nanocellulose; graphene oxide; hybrid aerogel; water purification; oil/water separation; adsorption). *Appl Env Biotechnol* 4(1):7. <https://doi.org/10.26789/aeb.2019.01.003>
- Wu C, Wang X, Zhuo Q, Sun J, Qin C, Wang J et al (2018) A facile continuous wet-spinning of graphene oxide fibers from aqueous solutions at high pH with the introduction of ammonia. *Carbon* 138:292–299. <https://doi.org/10.1016/j.carbon.2018.06.005>
- Xiong C, Zheng C, Nie S, Qin C, Dai L, Xu Y et al (2021) Fabrication of reduced graphene oxide-cellulose nanofibers based hybrid film with good hydrophilicity and conductivity as electrodes of supercapacitor. *Cellulose* 28(6):3733–3743. <https://doi.org/10.1007/s10570-021-03791-0>
- Xu J-T, Chen X-Q (2019) Preparation and characterization of spherical cellulose nanocrystals with high purity by the composite enzymolysis of pulp fibers. *Biores Technol* 291:121842. <https://doi.org/10.1016/j.biortech.2019.121842>
- Xu S, Yu W, Yao X, Zhang Q, Fu Q (2016a) Nanocellulose-assisted dispersion of graphene to fabricate poly(vinyl alcohol)/graphene nanocomposite for humidity sensing. *Compos Sci Technol* 131:67–76. <https://doi.org/10.1016/j.compscitech.2016.05.014>
- Xu Z, Liu Y, Zhao X, Peng L, Sun H, Xu Y et al (2016b) Ultrastiff and strong graphene fibers via full-scale synergistic defect engineering. *Adv Mater* 28(30):6449–6456. <https://doi.org/10.1002/adma.201506426>
- Xu T, Jiang Q, Ghim D, Liu K-K, Sun H, Derami HG et al (2018) Catalytically active bacterial nanocellulose-based ultrafiltration membrane. *Small* 14(15):1704006. <https://doi.org/10.1002/smll.201704006>
- Yan H, Tao X, Yang Z, Li K, Yang H, Li A et al (2014) Effects of the oxidation degree of graphene oxide on the adsorption of methylene blue. *J Hazard Mater* 268:191–198. <https://doi.org/10.1016/j.jhazmat.2014.01.015>
- Yan J, Dong K, Zhang Y, Wang X, Aboalhasan AA, Yu J et al (2019) Multifunctional flexible membranes from sponge-like porous carbon nanofibers with high conductivity. *Nat Commun* 10(1):5584. <https://doi.org/10.1038/s41467-019-13430-9>
- Yang J, Zhang E, Li X, Zhang Y, Qu J, Yu Z-Z (2016) Cellulose/graphene aerogel supported phase change composites with high thermal conductivity and good shape stability for thermal energy storage. *Carbon* 98:50–57. <https://doi.org/10.1016/j.carbon.2015.10.082>
- Yang M-C, Tseng Y-Q, Liu K-H, Cheng Y-W, Chen W-T, Chen W-T et al (2019) Preparation of amphiphilic chitosan-graphene oxide-cellulose nanocrystalline composite hydrogels and their biocompatibility and antibacterial properties. *Appl Sci* 9:3051
- Yavari F, Chen Z, Thomas AV, Ren W, Cheng H-M, Koratkar N (2011) High sensitivity gas detection using a macroscopic three-dimensional graphene foam network. *Sci Rep* 1(1):166. <https://doi.org/10.1038/srep00166>
- Yousefi N, Wong KKW, Hosseini Z, Sørensen HO, Bruns S, Zheng Y et al (2018) Hierarchically porous, ultra-strong reduced graphene oxide-cellulose nanocrystal sponges for exceptional adsorption of water contaminants. *Nanoscale* 10(15):7171–7184. <https://doi.org/10.1039/C7NR09037D>
- Yu H, Zhang S, Wang Y, Yin D, Huang J (2021) Covalent modification of Nanocellulose (NCC) by functionalized Graphene oxide (GO) and the study of adsorption mechanism. *Compos Interfaces* 28(2):145–158. <https://doi.org/10.1080/09276440.2020.1731276>
- Yu S, Yang Y, Zhu J, Ma L, Jia W, Zhou Q et al (2023) Wear and anticorrosive properties of graphene oxide-cellulose nanofiber composite coatings. *Mater Chem Phys* 128002. <https://doi.org/10.1016/j.matchemphys.2023.128002>
- Zhang J, Elder TJ, Pu Y, Ragauskas AJ (2007) Facile synthesis of spherical cellulose nanoparticles. *Carbohydr Polym* 69(3):607–611. <https://doi.org/10.1016/j.carbpol.2007.01.019>
- Zhang S, Geryak R, Geldmeier J, Kim S, Tsukruk VV (2017) Synthesis, assembly, and applications of hybrid nanostructures for biosensing. *Chem Rev* 117(20):12942–13038. <https://doi.org/10.1021/acs.chemrev.7b00088>
- Zhang Y, Peng J, Li M, Saiz E, Wolf SE, Cheng Q (2018) Bioinspired supertough graphene fiber through sequential interfacial interactions. *ACS Nano* 12(9):8901–8908. <https://doi.org/10.1021/acs.nano.8b04322>
- Zhang L, Yu Y, Zheng S, Zhong L, Xue J (2021) Preparation and properties of conductive bacterial cellulose-based graphene oxide-silver nanoparticles antibacterial dressing. *Carbohydr Polym* 257:117671. <https://doi.org/10.1016/j.carbpol.2021.117671>
- Zhang Y, Wei L, Liu X, Ma W, Lou C, Wang J et al (2022) Tromethamine functionalized nanocellulose/reduced graphene oxide composite hydrogels with ultrahigh gravimetric and volumetric performance for symmetric supercapacitors. *J Power Sources* 543:231851. <https://doi.org/10.1016/j.jpowsour.2022.231851>
- Zhang L, Deng K-K, Nie K-B, Wang C-J, Xu C, Shi Q-X et al (2023) Thermal conductivity and mechanical properties of graphite/Mg composite with a super-nano CaCO₃

- interfacial layer. *iScience* 26(4):106505. <https://doi.org/10.1016/j.isci.2023.106505>
- Zhao Y, Li J (2014) Excellent chemical and material cellulose from tunicates: diversity in cellulose production yield and chemical and morphological structures from different tunicate species. *Cellulose* 21(5):3427–3441. <https://doi.org/10.1007/s10570-014-0348-6>
- Zhao M-Q, Zhang Q, Huang J-Q, Tian G-L, Nie J-Q, Peng H-J et al (2014) Unstacked double-layer templated graphene for high-rate lithium–sulphur batteries. *Nat Commun* 5(1):3410. <https://doi.org/10.1038/ncomms4410>
- Zheng C, Yue Y, Gan L, Xu X, Mei C, Han J (2019) Highly stretchable and self-healing strain sensors based on nano-cellulose-supported graphene dispersed in electro-conductive hydrogels. *Nanomaterials* 9(7). <https://doi.org/10.3390/nano9070937>
- Zhu Y, Murali S, Cai W, Li X, Suk JW, Potts JR et al (2010) Graphene and graphene oxide: synthesis, properties, and applications. *Adv Mater* 22(35):3906–3924. <https://doi.org/10.1002/adma.201001068>
- Zhu W, Li W, He Y, Duan T (2015) In-situ biopreparation of biocompatible bacterial cellulose/graphene oxide composites pellets. *Appl Surf Sci* 338:22–26. <https://doi.org/10.1016/j.apsusc.2015.02.030>
- Zhu Q, Ong PJ, Goh SHA, Yeo RJ, Wang S, Liu Z et al (2023) Recent advances in graphene-based phase change composites for thermal energy storage and management. *Nano Mater Sci*. <https://doi.org/10.1016/j.nanoms.2023.09.003>
- Zmejkoski DZ, Marković ZM, Mitić DD, Zdravković NM, Kozyrovska NO, Bugárová N et al (2022) Antibacterial composite hydrogels of graphene quantum dots and bacterial cellulose accelerate wound healing. *J Biomed Mater Res B Appl Biomater* 110(8):1796–1805. <https://doi.org/10.1002/jbm.b.35037>

Publisher's Note Springer Nature remains neutral with regard to jurisdictional claims in published maps and institutional affiliations.